



Universidad
del País Vasco

Euskal Herriko
Unibertsitatea

ZIENTZIA
ETA TEKNOLOGIA
FAKULTATEA
FACULTAD
DE CIENCIA
Y TECNOLOGÍA



Bachelor thesis/ Gradu amaierako lana/ Trabajo fin de grado
Physics Degree/ Fisikako gradua/ Grado en Física

Development of an immersion microscopy technique on ice
Izotzarentzako inmertsio mikroskopia teknika baten garapena
Desarrollo de una técnica de microscopía de inmersión para el hielo

Author/ Egilea/ Autor/a:
Bittor Muniozguren Arostegi
Directors/ Zuzendariak/ Directores/as:
Sérgio H. Faria
Gabriel A. López

Leioa, 26th july 2022/ Leioa, 2022eko uztailaren 26a / Leioa, 26 de julio de 2022

Summary

Despite of being called the blue planet, fresh water constitutes just a small fraction of all water available on Earth. About three quarters of this fresh water is stored as ice and snow all around the globe, mainly on glaciers and on ice sheets at the poles. Besides being the water towers of the world, this perennial ice contains internal structures and impurities that serve as an archive of the climate history of the planet. Nevertheless, the integrity of this record is conditioned by the dynamics of ice. Ice microstructures are constantly under the influence of the ice inner flow (also called “creep”), which also influences the ice melting and the rise of sea level. In order to study the marks that the ice creep leaves on its microstructure, optical microscopy is often used. The aim of this work is to assess the viability of oil immersion microscopy on the study of ice microstructures. Immersion microscopy, which consists of using an oil between the objective lens and the specimen, is a technique well-developed for the study of diverse materials, but it has so far not been explored for the study of ice. As described in this work, this technique might bring certain advantages, e.g., a higher resolution. On the other hand, certain challenges may appear, including problems with immersion oils at low temperature and absence of information about how different oils react to low temperatures. In order to overcome these problems dimethicone was used (historically used to preserve ice samples and does not change dramatically at low temperature) and the absent information (viscosity and refraction index) was roughly calculated. The results can be divided in two categories: the observation of surface structures, which seems to give better photomicrographs through traditional "dry" microscopy, using a combination of incident and transmitted illumination; and intracrystalline structures, which gives notably better images through immersion microscopy, using transmitted light only. The quality of these last results encourages us to believe that immersion microscopy has a huge potential on ice as a complementary technique for traditional "dry" microscopy.

Acknowledgements

I would like to express my special thanks of gratitude to both of my co-directors on this project, Sérgio H. Faria and Gabriel A. López, who gave me the opportunity to do this project and guided me during all the process. I would also like to convey my heartfelt appreciation and gratitude to Patricia Muñoz Marzagón (technical manager at the IzotzaLab) for the invaluable help she has offered so this work could be done. I also wish to thank Nicolás Gonzalez Santacruz for providing the ice samples used in this research, as well as to all the IzotzaLab and BC3 for accepting me with such kindness. Once again I would like to thank Sérgio and Patricia for the opportunity of participating in the "International Symposium on Ice in a Sustainable Society", where a poster based on this work was awarded the prize as the best poster. Finally I would like to thank all the people that had any kind of participation at this work and were not included above.

Index

1	Introduction and objectives	1
1.1	Ice on our planet	1
1.1.1	Ice structure	3
1.1.2	Techniques to study ice structure	6
1.2	Immersion microscopy	7
1.2.1	History	7
1.2.2	Basic concepts of light physics	8
1.2.3	Basic concepts of microscopy	9
1.2.4	Oil immersion objectives and microscopy	11
1.3	Objectives	12
2	Development	13
2.1	Advantages and challenges of immersion microscopy on natural ice	13
2.1.1	Measurement of the viscosity of the oil	15
2.2	Methodology to study ice structure by immersion microscopy	21
2.2.1	Determining the aim of the study and the cut	21
2.2.2	Preparation of the sample	22
2.2.3	Selection of a point of interest using traditional objective lenses	23
2.2.4	Applying the oil and observation by an immersion objective lens	24
2.3	Results of immersion microscopy and comparison with traditional microscopy	25
2.3.1	Surface structures	25
2.3.2	Inner structures	29
3	Conclusions	33
	References	35

1 | Introduction and objectives

1.1 Ice on our planet

Water (H_2O) is one of the most familiar substances on our planet. Moreover, it is responsible for one of its best known nicknames: the blue planet. Even if sometimes its liquid form attracts most of the attention, its solid form, i.e., ice, turns out to be very interesting for a variety of areas such as geology, thermodynamics, solid state physics, climatology, and environmental sciences.

Ice can naturally exist in a number of forms, e.g., snow, glaciers and ice caps, ice sheets, ice shelves, sea ice, river and lake ice, and frozen ground (permafrost). All these ice forms collectively constitute the cryosphere of our planet. One might directly think of the poles when talking about natural ice¹ (Antartica stores 90% of the ice of the planet, which is about 65% of world's freshwater), but ice actually exist all around the globe. Big ice reserves can be found in the glaciers in Alaska (about 5% of the state is covered with glaciers), Altai-Sayan glaciers (over 2,000 glaciers in southern Siberia and North-western Mongolia), Andean glaciers (the tropical part of the Andes contain more than 99% of all tropical glaciers), Glaciers of the Karakoram Himalaya (some of the largest valley glaciers outside high latitudes and a total of over 5,000 individual glaciers), Caucasus mountains (over 2,000 glaciers particularly on north facing slopes), Greenland (on one hand, we have the Greenland Ice Sheet, which covers 80% of the island, but, on the other hand, we have many glaciers outside the ice sheet), Himalaya (as the highest mountain range on our planet, constitutes a huge repository of snow and ice), Kunlun mountains (6,580 glaciers in western China) or the Alps (alpine glaciers occupy an extension of about 2,900 km² in the hearth of Europe) (Bishop et al., 2011).

Even if many of those regions are slightly populated, the cryosphere has a massive impact on the lives of millions of people all over the globe. The snow, ice and glaciers of the highlands may have a massive impact on far away areas, because the meltwater from mountain areas feeds rivers from populated lowlands. This is the case of the Alps and rivers such as the Rhine, the Rhone and the Po. Glaciar structures act as control systems so that the water supply remains regular during spring and summer, avoiding droughts. Keeping a regular water runoff is absolutely necessary for many socioeconomic activities such as the production of energy, agriculture and industry. Moreover, the cryosphere contains about three quarters of the Earth's fresh water, so glaciers and ice are, in fact, sweet water storage structures, essential for every living being on the planet (Barrenetxea and Faria, 2022).

The cryosphere also plays an important role regulating global climate. Snow and ice, due to their white colour, reflect most of the solar radiation in snow-covered areas, unlike darker surfaces such as the sea or soil, that absorb that heat. The percentage of reflected radiation by a surface in relation to the incident radiation is known as albedo. A sustainable ratio of high and low albedo areas, alongside with the natural greenhouse effect of the atmosphere is essential to regulate global temperature. In fact, the Earth is a natural greenhouse, which means that certain gases of the atmosphere allow solar radiation

¹We refer as natural ice to any naturally formed ice that has been extracted from low temperature areas of the world. On the other side, artificial ice is the ice produced in a freezer.

to reach the Earth's surface, but absorb and re-radiate part of the outward infrared radiation. This phenomenon is essential for the habitability of the Earth. Nevertheless, the massive emissions of greenhouse gases by human activities lead to a strong increase of the greenhouse effect and a rapid global warming. Rising temperatures may affect especially high-altitude ground and high latitudes, severely damaging the cryosphere. The melting of the poles, sea ice and mountain snow would lead to replace those white areas with darker colour areas such as navy blue water and brown or grey soil. This may lead to these areas absorbing larger amounts of infrared radiation and maximising global warming. Sea ice not only affects global climate due to its high albedo, but it also conditions the exchange of energy between the atmosphere and the ocean, influencing the global heat balance.

A widely known consequence of global warming and the melting of the cryosphere is the potential rising of the global sea level. If all the ice in Antarctica melted, it would raise the worldwide sea levels by 60 or 70 meters (Bishop et al., 2011). In order to analyse this danger it is important to remember that the ice sheet surface itself is around 3,000 meters above the mean sea level (MSL) in the interior of the continent. This elevation does not make surface melting very likely in the interior of the continent (although basal melting may occur at the bottom ice-rock interface). So, as it happens with the glaciers, ice is not melting homogeneously, but ice flows on this macroscopic structures, following the bedrock and its own slope, ending at a lake or the sea. This flow, known as creep, is a high-temperature plastic deformation on a solid, forcing it to flow like a highly viscous fluid. Creep occurs above a certain temperature and is characteristic of polycrystalline solids. As all the cryosphere is relatively close to ice melting temperature, this phenomenon is present in every natural structure formed by ice. The flow of the ice, little by little affects its microstructure, which can be studied in order to determine how the ice macrostructures behave. As if they were scars, the deformations and irregularities in the crystal lattice of the ice can be read, to understand the behaviour of Antarctica or other glaciers, so that it can give some clues of how the ice is reacting to the global warming (Faria et al., 2017).

Moreover, the study of natural ice not only leads to understanding the dynamics of the cryosphere, but also allows us to read the ice structure as a paleoclimatic record. The inclusions, microinclusions, bubbles and clathrate hydrates allow us to study the atmospheric circumstances over the history. Snowflakes are accumulated on the surface of polar areas during snowfalls and form a porous medium that allows air to move inside. With new snowfalls, lower layers compact and snow turns into ice, enclosing and isolating air bubbles, preserving a sample of the aerosols of the atmosphere at the time. Unfortunately, these samples are not preserved as independent layers, but are affected by the inner flow of the ice that we have already mentioned. In order to determine in which way has the ice flow affected the integrity of the paleoclimate records, microstructure mapping is used, alongside with ice core line-scanning.

To sum up, ice awakens interest in many areas of study due to its crystalline structure, as a tool to understand climate change or global heat balance or due to its utility as a record of the climate conditions over the history, but all of them have in common the need to analyse its microstructure.

1.1.1 Ice structure

Ice is formed of water molecules (H_2O) arranged in a crystalline pattern. Even if ice can have circa 12 different crystalline phases, the only stable phase on Earth's surface is the hexagonal arrangement pattern. This phase is known as ice *1h* and its hexagonal symmetry even affects structures that are on a larger scale than the crystal pattern; for example, the snow crystals (Faria et al., 2014). Nevertheless, our focus here is not the analysis of the regular crystal pattern of ice. Instead of that, our focus is kept at larger scale structures derived from irregularities in the crystal lattice or at inclusions such as bubbles. So, somehow the study of ice microstructure consists more in analyzing the imperfections and deformations of the regular structure than on analysing the regular structure itself, as those irregularities are what characterise the ice deformation and store the climate records. We need to remember that the reasons to study ice microstructure are to determine the circumstances that our samples suffered, in order to understand in which way had that sample flown or in which climatic conditions it crystallized. Even at risk of over trivializing the ice structure analysis, we could say that we mainly look for those distinguishing factors that are the ones telling the story of each ice sample.

In order to get into detail, we are now going to clarify the different scales of ice microstructure (Faria, 2009):

- **Phase structure:** Is the largest scale structure when a polycrystal² is analyzed. This study of the structure distinguishes different substances than cannot be chemically combined, known as phases, and these phases can be polycrystals themselves or just monocrystals. They also have to be included on the phase structure all the inclusions on the ice, as they are different substances, even if often are smaller than grains. Bubbles or clathrate hydrates³ are examples of inclusions.
- **Grain structure:** When a number of ice polycrystals that are at the same phase are found together, we can talk about grain structure, each of those crystals been called a grain. Each grain is formed by a regular crystal pattern, but the lattices from different grains are misaligned, therefore, the crystal lattice at the borders of the grains is not bonded as well as at the rest of the crystal, i.e. a grain boundary is formed.
- **Substructure:** Is complementary to the grain structure and is formed by those formations that can be found inside each of the grains. Their size is at the order of 10 angstroms, so they cannot be directly seen through the microscope. Dislocations and vacancies are examples of the substructure or defects.
- **Crystal structure:** Is related to the position of atoms at the unit cell of the lattice. This structure is at an even smaller scale than the previous one, of the order of the angstroms, so it can neither be studied by optic microscopy.

²**Polycrystal:** Material formed by simple crystals of the same substance. These simple crystals are often named grains.

³**Clathrate hydrate:** Crystalline lattice forming cage-like structures that enclose other molecules.

A key point for the microstructure is that it is not perfect. A perfect crystal would be at equilibrium and would be absolutely static, but ice has some defects, which lead to a dynamic structure. Defects appear at different moments such as crystallization or deformation and, due to their instability, they force the lattice to evolve (in order to reduce the free energy stored in the defects). Below are a few examples of defects that have been categorised according to their dimensions (Faria, 2009):

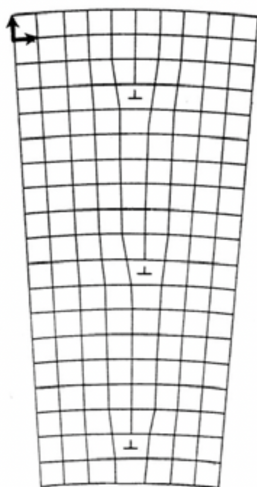


Figure 1: Illustration of a grain boundary. Several mismatches of the two misaligned crystal lattices can be observed (Humphreys and Hatherly, 2004).

- **Vacancies** are dimensionless defects, as consist of the absence of a molecule of the crystal lattice.
- **Dislocations** are line defects formed due to a mismatch of the crystal lattice. Dislocations have the ability to move trough the crystal and may absorb vacancies. An accumulation of this kind of imperfections on a grating or grid may potentially form a subgrain boundary and evolve into a grain boundary.
- **Grain boundaries** are two-dimensional defects formed by a considerable misalignment of the lattice of two grains. Inside a single crystal or grain we can also find similar alterations of the lattice at an angle small enough to avoid creating two different grains. This misaligned lattices are known as subgrains and the border would be a subgrain boundary.

It should be reiterated that the ice microstructure is dynamic, which leads to these defects evolve from one category to another.

The crystal defects that force the instability and, therefore, the dynamics of ice structure, can directly affect the evolution of the polycrystals. Indeed, a grain with a high amount of dislocations should tend to reduce its size while a grain with a low number of dislocations shows a tendency to grow.

The crystals of the ice can evolve due to different phenomena, e.g., dislocations coming together and absorbing vacancies to form subgrain boundaries is called recovery. These defects can keep growing and afterwards develop to grain boundaries, which is known as recrystallization. This phenomenon will tend to increase the number of grains (Faria et al., 2017).

On the other hand, we also have normal grain growth (NGG), which can be observed when a polycrystal is let evolve exclusively by minimization of the grain boundary energy (this occurs when the energy stored in other defects is negligible). In the two dimensional case, it is based on the stability of the hexagon as the stable surface-filling polygon, so all the polygons with less than six sides will lose sides and shrink until they disappear and

the ones with more than six sides will grow and reduce sides until they become hexagons. If some grains disappear, then inevitably the mean size of the bidimensional crystals must have increased. In the two dimensional case it is theoretically possible to reach an stable structure formed by identical regular hexagons, but in the three dimensional case there is no such a polyhedron that would allow the equilibrium of the three-dimensional grain-boundary network. Consequently, NGG in three dimensions would theoretically continue until all grain boundaries disappear. In practice, normal grain growth coexists with many other phenomena and its effect is much more difficult to identify (Faria, 2009).

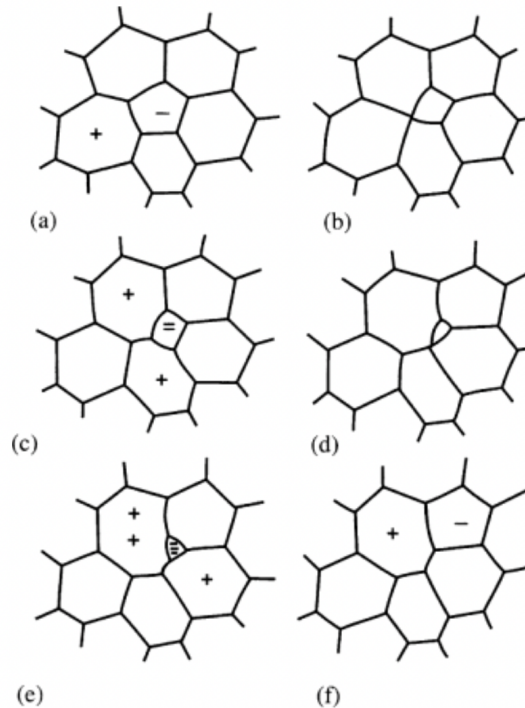


Figure 2: General scheme of normal grain growth on two dimensions. The pentagon in the middle shrinks until disappearing, making the mean size of the grains grow (Humphreys and Hatherly, 2004).

Normal grain growth, recrystallization and other alterations of grain structure are some of the phenomena analyzed in order to understand the dynamics of the ice. When using the microscope, the structures on the scale of grains are observed, like e.g., inclusions, bubbles, grain and subgrain boundaries. It must be said, however, that the ice grain and subgrain boundaries themselves are narrower than the resolution of the microscope. Nevertheless, the bond energy between the molecules of the crystal lattice is much weaker at the boundaries (that is, the bonds are distorted near the boundary), as the lattice is not well-formed in there. This implies that the zones where grain boundaries meet the surface of the ice sample will have a higher sublimation rate than the rest of the ice surface. Therefore, sort of a groove will be formed along the points where the grain boundary meets the ice surface, which is observable at the microscope (Kipfstuhl et al., 2006).

1.1.2 Techniques to study ice structure

Traditionally, the ice structure has been studied through optical microscopy. The low temperature needed to preserve the ice samples can cause problems on complex equipment; that is why the simplicity and robustness of traditional optical microscopy may bring an advantage against potential malfunctioning. More intricate systems might be more demanding in terms of ambient conditions in which they can work.

The most common objective lenses used in optical microscopy are "dry" objective lenses, which work with air between the specimen and the lens. Nevertheless, there is another type of lens which demands a liquid environment (usually some type of oil) between the specimen and the objective lens. A high viscosity oil is spilled on the surface that we want to observe and when we plunge the point of the objective into the oil a meniscus is formed. The surface tension will maintain the meniscus stable and we will have substituted the air layer by a medium with higher refractive index. The technique of using an oil objective is called immersion microscopy and will be described in detail later.

To our knowledge, there is no previous study that shows any attempt to use immersion microscopy at such as low temperature to study ice structures. That might lead to some scepticism, but a hypothetical approach to our proposition leads us to believe that this technique could offer certain advantages:

1. On the laboratories that work with natural ice, prepared ice surfaces are often covered with a thin coating of transparent silicone oil, to protect them against the elements. So, in this case, instead of substituting the air layer with oil, it would be more like eliminating a layer (air), if we find an oil that can do both assignments. In any change of medium, light suffers refraction, so the elimination of a layer, and thus the elimination of a refractive surface may be an advantage in favor of immersion objectives.
2. Immersion microscopy is supposed to reduce reflections that derive from spurious incident light. So, if, for any reason, we have a problem with reflections, immersion microscopy might be a good alternative.
3. Due to the high refractive index of the immersion oil, the light beams coming from the sample do not scatter as much as on the air. Therefore, immersion objective lenses have a higher resolution power, which might not be determinant for mapping the structure of a complete ice sample, but might give an advantage when we want to study a specific point in higher detail, such as a microinclusion, a clathrate hydrate or a bubble.

1.2 Immersion microscopy

Inspection by sight is one of science's oldest, yet most useful ways to study the world that surrounds us. Nevertheless, human sight is quite limited and in order to overcome those limitations, many advances in optic devices have been made such as microscopes or telescopes. We are interested in magnification optical devices, as the aim of this work will be to study the microstructure of ice. From the first simple hand lenses to modern microscopes, these tools have evolved to satisfy the needs of many areas of study, always aiming the direct observation of microscopic samples.

1.2.1 History

Even though simple lenses had been documented many centuries ago, it was not until the late sixteenth century and the early seventeenth century that the first compound microscopes appeared. Some spectacle makers were supposed to combine a convex lens with a concave lens around 1590 in the Netherlands. This crude compound microscope was later known as the Dutch microscope. Two decades later, this invention inspired Johann Kepler (1571-1630), who concluded that the combination of two convex lenses would also lead to a microscope that provided upside down images.

Cornelis Drebbel (1572-1633), who was also from the Netherlands, was another relevant character in the history of microscopy. In 1619, a compound microscope was documented in his possession in London. The Dutch inventor had created a system formed by a biconvex ocular and a plano-convex objective alongside with a diaphragm. This instrument was studied by Galileo Galilei (1564-1642) in 1624. Galilei had already used a telescope at close range to achieve the enlargement of images almost 15 years before, for which is sometimes recognised as the inventor of the microscope. He had access to the compound microscope built by Drebbel when it was exhibited in Rome and worked to create his own improved version of it.

Later on the seventeenth century, Robert Hooke (1635-1703) tried including a third lens between the objective lens and the ocular lens. He concluded that the relative position of the middle glass affected the magnification of the optic system. Following the precedents set by Hooke, Antony von Leeuwenhoek (1632-1723) created more than 400 microscopes, with a range in magnification from 69x to 266x and in numerical aperture from 0.11 to 0.37. This hand-held prototypes evolved into table microscopes and continued their evolution developing advances in illumination or aberration correction (Rochow and Tucker, 1994).

Looking for a solution to reduce chromatic aberrations, Giovanni Amici (1786-1863) first developed water and oil immersion objectives. To finish with the acknowledgement of the most relevant improvements in the history of microscopy, Ernest Abbe (1840-1905) has to be mentioned. Not only he created improved versions of Amici's oil immersion objectives, but his work in many aspects of microscopes, such as the illumination, alongside with his advances in theoretical concepts as the numerical aperture were fundamental for the development of microscopy (Ockenga, 2015).

1.2.2 Basic concepts of light physics

Before we go on with optical microscopy, it is important to remember that these optical devices are tools that allow us to overcome limitations of the human eyesight. In other words, microscopes are a way to manipulate light in our benefit. Therefore, some light related phenomena have to be studied in order to fully understand immersion microscopy. We have already mentioned that immersion microscopy uses oil between the specimen and the objective, so, understanding refraction, reflection and the dependency of the speed of light on the propagation medium will be determinant not only to predict the advantages of the immersion microscopy on ice, but also to evaluate the different illumination techniques.

Visible light is an electromagnetic wave with a frequency between 380 and 750 nanometres, which, even if it does not need a material medium to propagate, it is indeed conditioned by the medium. The speed of light in vacuum is 299,792,458 m/s (Baird et al., 1979) and will be lower in any other material medium. Therefore, we can relate the speed of light (c) in vacuum with that in any other medium (v_i). This parameter is known as the refraction index (n_i).

$$n_i = \frac{c}{v_i} \quad (1)$$

Note that this parameter will always be higher than one, as the speed of light in any material medium will be lower than the speed of light in vacuum.

When light arrives at the interface between two media, part of the light returns to the medium where the incident light was coming from and another part crosses to the second medium. These two phenomena receive the names of reflection and refraction, respectively. Figure 3 introduces a scheme in order to remember these notions.

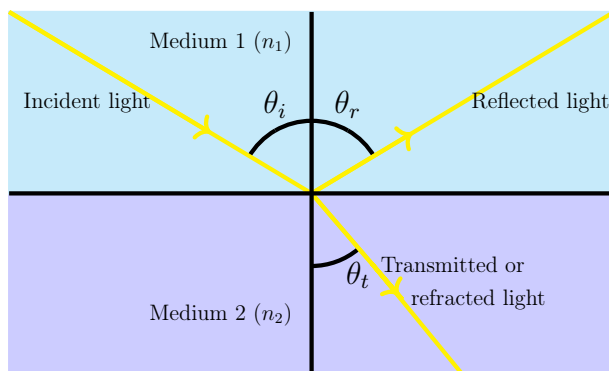


Figure 3: Incident, reflected and refracted (or transmitted) light shown in the plane of incidence.

The dependency of the angles on the relation of the refraction indexes is described by Snell's law in the following equation:

$$n_1 \cdot \sin(\theta_i) = n_2 \cdot \sin(\theta_t) \quad (2)$$

where θ_i and θ_t are the angle of the vertical and incident and transmitted light beams, respectively.

So this dependency on the refraction indexes allows us to predict that high refraction index media, such as oil would lead to smaller refraction angles, which is highly related to the numerical aperture and the resolution, that we are going to explain in detail later on.

It is also important to describe the intensities of the reflected and transmitted light as a function of the refraction indexes and the intensity of the incident light to understand how different ways of illumination might affect to the "dry" microscopy and the immersion microscopy. As the intensity is proportional to the square of the module of the amplitude, the Fresnel equations must be studied to determine the amplitudes. As the objectives are vertically located above the samples and the point of interest should be in the centre of the image, we consider the special case of the Fresnel equations for the normal incidence (Born and Wolf, 2013):

$$T_{\parallel} = \frac{2}{n+1}A_{\parallel} \quad T_{\perp} = \frac{2}{n+1}A_{\perp} \quad (3)$$

$$R_{\parallel} = \frac{n-1}{n+1}A_{\parallel} \quad R_{\perp} = -\frac{n-1}{n+1}A_{\perp} \quad (4)$$

where A_{\parallel} , T_{\parallel} and R_{\parallel} are the components of the amplitude that are parallel to the plane of incidence for the incident, refracted and reflected beams, respectively. In the same way A_{\perp} , T_{\perp} and R_{\perp} are the components of the amplitude that are perpendicular to the plane of incidence and $n = \frac{n_2}{n_1}$.

To compare the incident intensity with that of the reflected and transmitted light two parameters are defined: transmissivity (\mathcal{T}) and reflectivity (\mathcal{R}).

$$\mathcal{T} = n \frac{|T_{\parallel}|^2}{|A_{\parallel}|^2} = n \frac{|T_{\perp}|^2}{|A_{\perp}|^2} = \frac{4n}{(n+1)^2} \quad \mathcal{R} = \frac{|R_{\parallel}|^2}{|A_{\parallel}|^2} = \frac{|R_{\perp}|^2}{|A_{\perp}|^2} = \left(\frac{n-1}{n+1}\right)^2 \quad (5)$$

So, in the different medium limits, the difference between the two refraction indexes might condition if observing reflected, transmitted or reflected and transmitted light simultaneously gives higher or lower quality images. However, other parameters such as the contrast may also have an important role. What the transmissivity and reflectivity definitely suggest is that if there are several media between the sample and the objective, as in the case of a protection glass and the oil used for immersion microscopy, the closer their refraction indexes are the better will be the quality of the image. In case we achieve those indexes to be the same, a potential loss of intensity would be avoided.

1.2.3 Basic concepts of microscopy

The categorization and operation of microscopes and objective lenses is conditioned by a number of concepts that will now be explained.

Magnification

It defines the size relation between the image and the sample. The magnification power is dimensionless but it is written with an "x" next to the value, for example 5x, meaning that this optical system will give an image five times bigger than the size of the object.

An optical system can be formed by the connection of several optical systems. The microscope itself is a system where we connect an ocular and an objective. As the magnification of the ocular will affect to the image that the objective has already magnified, we can easily conclude that the total magnification power of connected optical systems will be the power of the magnification of the individual systems. In the case of digital images, digital zoom could lead to a confusion. Therefore we are going to use the magnification power to define the scale of the image and define the size in absolute terms (e.g., in micrometers).

Finally, and even if it can seem obvious, the magnification should be homogeneous in all directions. If it is not, the image will be deformed and apparent proportions and shapes would not be real.

Numerical aperture

Numerical aperture (NA) is a parameter used to describe the ability of the lens to gather light. In traditional objective lenses can be understood as the size of the cone formed by the light that can reach the objective. So, an objective lens with a high numerical aperture has a larger light entry cone than the ones with a low NA . Formally, it is not only conditioned by the size of the light cone that can enter the objective but also by the refraction index between the optics and the sample. Therefore, its value can be calculated in the following way (Rochow and Tucker, 1994):

$$NA = n \cdot \sin(\theta) \quad (6)$$

where n is the refraction index of the intermediate medium and θ is half of the angle of the vertex of the cone.

A narrow cone of light (a low NA) means that photons are concentrated in a smaller area, so the image will seem brighter. On the other hand, a wide cone of light (a high NA) means that photons are spread over a larger area and, therefore, the images will be darker. Normally, this limitation can be easily overcome regulating the light source.

The condenser also is characterised by a numerical aperture. In this case, it is not the light that can gather, but the cone of light that it creates. A condenser with a high NA creates a large light cone and a low NA leads to a narrow light cone.

The total aperture angle (half the angle of the light cone) of the objective and the condenser is the sum of the independent aperture angles.

Resolution

The resolution of an objective lens is the distance needed between two adjacent objects to distinguish them as two independent identities. So the higher the resolution is the more the details seen in the images will be.

The limit of resolution can be calculated with the following equation (Lawlor, 2019):

$$R = \frac{\lambda}{2 NA} \quad (7)$$

where λ is the wavelength of the light used.

The resolution has acquired quite an importance in the era of digital images, as in digital images zoom can be used to compensate optical magnification, if the resolution is high. It can be seen at the formula (7) that resolution has no dependency on magnification, therefore a low magnification image with a high resolution could be magnified and might obtain better results than a higher magnification image with a poor resolution.

Focus

An image is formally considered in focus when all the details of the image are well defined. Ideally, in any microscopy technique, the eye should be relaxed and all the effort should be done using the lenses of the microscope. The aim will be to find the correct distance between all the objects that form the optic system so that it gives the best image possible. Even though we focus our eyes intuitively, setting the microscope in focus is sometimes more tedious. Nevertheless, setting a correct focus is crucial, especially when we are going to make use of the digital magnification that we have previously mentioned. Even if the resolution of the microscope is fantastic, if the image is out of focus it will have poor detail definition and will be very notorious when magnified.

1.2.4 Oil immersion objectives and microscopy

Objectives are one of the most important elements of the optical microscope. It is partially responsible of the magnification and its characteristics will highly condition the results obtained at the microscope.

Objective lenses are intricate systems formed by high quality lenses, but can generally be described with a reduced series of parameters. Two of the main numerical data that characterise an objective lens are the numerical aperture and its magnification, which we have already seen in the previous section and are commonly expressed at the objective. Another key point when classifying objectives is whether it is an air or an oil objective. This qualitative characteristic determines if the system will need air or oil between the objective and the sample. Immersion objectives are characterised by a higher NA and, therefore, usually give higher resolution images. If we bring back equation (6), it seems obvious that with air, the maximum theoretical value will be 1, as the refraction index of the air is one. In the case of oil, the refraction index is higher, so the numerical aperture may reach values of 1.3, 1.4 or even 1.6 in some extreme cases (Rochow and Tucker, 1994).

We may also take into account that immersion objectives are only produced with high magnifications. We have previously mentioned that resolution is not conditioned by the magnification, but a powerful magnification will not have any advantage without a great resolution. Therefore, oil objectives are normally built with high magnifications as they assure good resolution, while air objectives can go from extremely low magnifications to magnifications similar to those of oil objectives.

In the case of our immersion objective lens (HC Pl FLUOTAR 63x/1.3 OIL), as it can be seen in Figure 4, the magnification and numerical aperture are 63x and 1.3, respectively (Leica-Microsystems). Anyways, note that the NA is not an intrinsic property of the objective, instead it is conditioned by the refraction index of the medium. The NA of this objective has been calculated for the exact refraction index of the oil produced by Leica, which also produced the optics, but if another oil is used, the NA could differ.

1.3 Objectives

The main objective of this work is to determine the advantages and usefulness of the immersion microscopy technique for the study of ice microstructures at low temperatures.

Several factors affecting the immersion microscopy will be tested in this work. One of them is related to the illumination of the sample. The illumination can be incident light, which gets the images from the light reflected at the sample; transmitted light, which gets them from the light refracted through the sample; or a combination of both. We may also take into account the use of polarized light and how it affects the resulting image. Another key factor for microscopy is whether the target of study is at the surface of the ice sample or if it is an intracrystalline structure. As the change from air to oil is reducing the refraction index difference, and therefore the refraction itself at the surface of the sample, this factor may be worth to analyse. So, among the high number of combinations given by these factors, we will aim to find those that show the most advantages.



Figure 4: The immersion objective lens used for this study.

In addition to the main objective already mentioned, this work has several other aims.

This project is developed in the context of the study of ice microstructure, so in order to evaluate the viability and usefulness of this technique, the interests of analyzing ice at a microscopic level are worth studying, alongside with some basic notions of ice microstructure. This objective is twofold. It may involve an initial theoretical approach, focused on internalizing the motivation of studying ice microstructure and the concepts related to it. Nevertheless, this objective also includes an experimental approach, in order to get used to the study of ice microstructures either through traditional optical microscopy or immersion microscopy.

Finally, in despite of this work leaving many aspects for further studies, one of its aims is to set a basis so those potential studies can take place. In order to set a consistent basis the methodology needs to be rigorously described so it can be replicated in the future.

2 | Development

2.1 Advantages and challenges of immersion microscopy on natural ice

The biggest challenge related to the immersion microscopy technique might be related to the selection of a suitable immersion oil and the determination of its physical properties at low temperature. The industry of microscopy lenses already provides many types of immersion oils. Nevertheless, these oils can be very demanding in terms of the conditions in which they can be used, especially with the temperature range. For instance, the standard microscopy oil provided for our objective by Leica Microsystems, identified as Type N Immersion Liquid, is composed of ester oils and synthetic hydrocarbons that dramatically unmix and degenerate outside its ideal working conditions of 23 °C. Unmixing can occur even at positive temperatures close to 18 °C if it is stored under such a temperature for a prolonged period of time.

On the other hand, a thin layer of silicon oil (dimethicone) is often used to preserve ice samples and to prevent further sublimation. Polydimethylsiloxane (PDMS) or dimethicone is a silicone oil with a wide variety of applications in several industries such as the production of cosmetics or hydraulic fluids. Its molecular formula is $\text{CH}_3[\text{Si}(\text{CH}_3)_2\text{O}]_n\text{Si}(\text{CH}_3)_3$, where the index "n" defines the length of the polymer molecule, which in turn determines the viscosity of the oil. The bigger the n, the longer the molecule and the higher the viscosity. When commercialized, these oils are categorized by their kinematic viscosity at 25 °C, which is usually measured in mm^2/s , also known as centistokes (cSt). The stokes are the physical unit for the kinematic viscosity in the centimetre–gram–second system of units (CGS). Therefore, the criteria for distinguishing different dimethicones will be their viscosity at around 25 °C. For instance, the 100 cSt dimethicone will be that oil with a viscosity of 100 cSt at $T=25$ °C. The 100 cSt dimethicone is the one commonly used to protect and preserve the surface of ice samples.

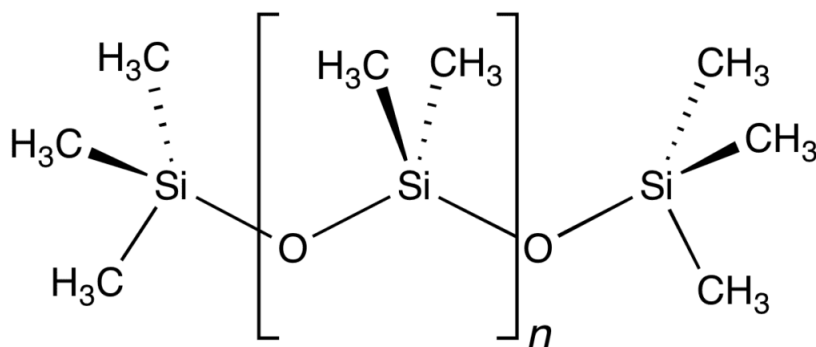


Figure 5: Two dimensional structure of a dimethicone molecule (Químicafácil, 2020).

Taking into account the above arguments, we conclude that our objective is finding a dimethicone oil that, at the low temperatures of ice microscopy (between -10 °C and -30 °C), reproduces the desired physical properties of the Leica Type N immersion oil at its ideal working temperature of 23 °C. There are mainly two physical properties that we are going to discuss to conclude if a dimethicone could accomplish the necessary conditions to

be used with the immersion objective: the refraction index and the viscosity.

First, we are going to discuss the refraction index. In certain cases, in biology for example, the sample is encased between two glasses, for preservation, preventing the oil from contaminating what we are observing. In those cases, the refraction index of the oil should be as similar as possible to the index of the glass, in order to avoid, as far as possible, the refraction caused by a change in the refraction index. In our particular case, there is no need to look for a match of indexes, as there is no intermediate medium between the ice and the oil. Our challenge is to determine the dimethicone that best reproduces at low temperatures (e.g. $-22\text{ }^{\circ}\text{C}$) the refraction index and viscosity of Leica Type N oil at its ideal temperature ($23\text{ }^{\circ}\text{C}$). A critical obstacle to achieve our objective is the fact that the producers' technical datasheets have little or no information about how dimethicones behave at very low temperatures. So, we only know the value of the refraction index at room temperature for both oils:

- $n_N=1.5180$ Leica Type N immersion oil ($T=23\text{ }^{\circ}\text{C}$ and 546.1 nm wavelength light) (Leica-Microsystems)
- $n_{100}=1.4030$ Dimethicone (100 cSt at $T=25\text{ }^{\circ}\text{C}$) (DOW, 2017)
- $n_{350}=1.4034$ Dimethicone (350 cSt at $T=25\text{ }^{\circ}\text{C}$) (DOW, 2017)

We can see that they are not equal at room temperature. Now, in the case of most organic liquids, the refraction index changes between -0.00035 and -0.00055 units per $^{\circ}\text{C}$ (UNAM). Dimethicone is an organic substance and it has shown no crystallization or other visual alterations at the cold temperatures of our laboratory (usually set to $-22\text{ }^{\circ}\text{C}$). Therefore, we are going to assume that dimethicone 100 cSt and 350 cSt are no exception to the above behaviour. As we do not exactly know the temperature coefficient for the refraction index of the dimethicone, we shall adopt the mean value, $-0.00045\text{ unit}/^{\circ}\text{C}$. Therefore, the expected refraction indexes at $T=-22.0\text{ }^{\circ}\text{C}$ of the dimethicone 100 cSt and 350 cSt are $n_{100(cold)}=1.4242$ and $n_{350(cold)}=1.4246$, respectively.

Even though the refraction indexes of the dimethicones are lower than we wished, they might be high enough to study the viability of the immersion microscopy with ice. As we have already mentioned, there is no protective glass, so this mismatch will not bring an intermediate refraction anyways. The only consequence expected for this difference on the indexes will be a resolution lower than the ideal one, but still notably higher than that achieved by the air objective lenses.

The other property that interests us about the oils are their viscosities. If the viscosity is too low the oil will spread rapidly and the oil layer will not be enough to immerse the objective. However, if it is too high, it will not spread correctly, so a big amount of oil would be needed to protect all the ice sample and the layer will be notably thick. Moreover, if the viscosity of the oil is too high, when the objective is moved, the friction between the oil and the ice could damage the sample. Therefore, if we need the oil for the immersion microscopy, but also to protect the sample, a well-balanced choice is needed. Even so, it is valuable to mention that we have a comfortable margin between those two limits.

If we take a look at the data available for the Leica Type N immersion oil, we get the following viscosity values at different temperatures (Leica-Microsystems):

- $\nu=1,060$ cSt at $T=20$ °C
- $\nu=825$ cSt at $T=23$ °C
- $\nu=295$ cSt at $T=37$ °C
- $\nu=245$ cSt at $T=40$ °C

As it happens with the refraction index, we are interested in finding a dimethicone oil with a viscosity at $T=-22$ °C close to that of the Leica Type N oil at $T=23$ °C.

2.1.1 Measurement of the viscosity of the oil

The oil was provided by the distributor Manuel Riesgo S.A., named as XIAMETER® PMX-200 Silicone Fluid. Forced by the absence of low-temperature information on the technical data sheets (DOW, 2017) of the oil, a simple experiment is proposed to roughly estimate the viscosity of the dimethicone oil.

The experiment consists on the emptying of a syringe full of this liquid and will be done twice: once at room temperature (18 °C) and another time inside the cold laboratory (-22 °C mean temperature). From now on, we are going to refer to the first one as the high-temperature experiment and to the second as the low-temperature one. The high-temperature experiment is just for quality control because the viscosity of the oil around 25 °C is provided by the datasheets.

As we are expecting to get a kinematic viscosity of 825 cSt at $T=-22$ °C, the dimethicone that we will use is a 350 cSt dimethicone. This decision is mainly based on the information provided by an old Bayer catalogue (Bayer), which states that their 350 cSt silicone oil would have a viscosity of 1,000 cSt at $T=-25$ °C (see Annex A). As the dimethicone oil is a pure substance, we expect the Bayer and the Xiameter dimethicones to behave similarly.

The experiment and its theoretical basis

The emptying of a syringe is a simple and straightforward way in which we can study the viscosity of a fluid. The emptying of a tube could be used also, involving easier calculations, but the experiment of the syringe is much slower. This helps minimizing the relative error of the time measurement, which is the most critical variable to obtain a satisfying result.

A clarification should be made in relation to the word "emptying". Indeed, we will not wait until the syringe is empty. As our aim is to measure viscosity, the study will only be valid while the oil is flowing and not dripping. In our experiment the gravity force on the oil itself leads to the flow, so that, as the syringe becomes empty, the gravity force produced by the oil column will not be strong enough to keep a flow and the remaining oil will begin to drip. The higher the viscosity, the sooner the dripping will start. Therefore, despite having the same starting condition, the high- and low-temperature experiments will not end at the same exact point. Each experiment ends just before the oil starts to drip.

In order to start with the analysis of fluid dynamics, some parameters related to the size and shape of the syringe must be defined. The syringe has 10 marks that indicate milliliters. Each time, it is filled above the tenth mark and we measure the time starting when the oil level passes the tenth mark until it reaches the mark of two or five milliliters, for the high- and low-temperature experiments, respectively.

The details of the instrumental have been measured with a caliper and are described in Figure 6 and Table 1, except for the r_0 , which is half d . Therefore, $r_0 = 1.010 \pm 0.05$ mm.

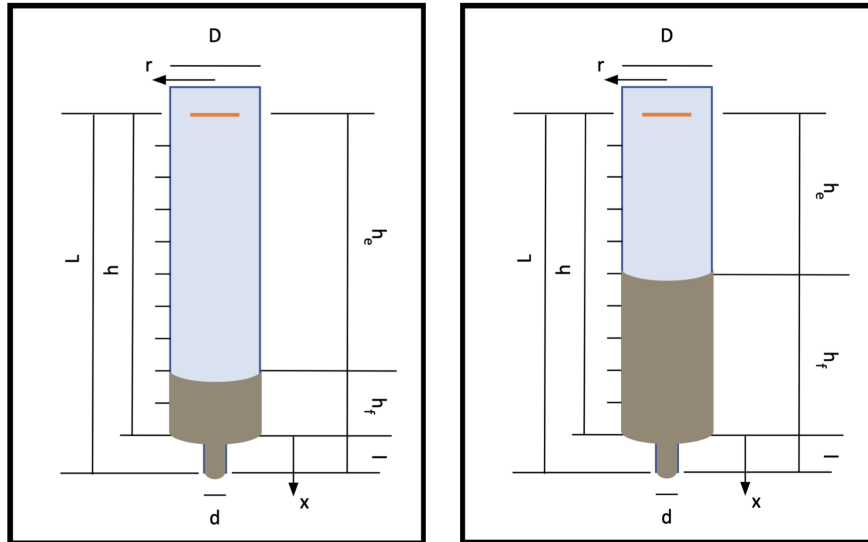


Figure 6: Dimensions of the syringe used in the experiments and the limit where the oil no longer flows and starts to drip, for the high- and low-temperature experiments from left to right, respectively.

Table 1: Values of the dimensions of the syringe of the experiments and the limit where the oil no longer flows and starts to drip. The instrumental error of all the measurements is 0.01 mm.

Parameter	Size (mm)	Parameter	Size (mm)
D	13.41	h_e (high)	52.05
d	2.02	h_f (high)	18.35
L	76.65	h_e (low)	32.43
l	6.25	h_f (low)	37.97
h	70.40		

Now we can go on analyzing the variables that we are directly going to measure and how they relate to the viscosity. The emptying of a syringe-shaped and steady container is characterised by a pressure only depending on the vertical position (x). Therefore, the equilibrium equation, taking into account the shear stresses (τ) at the mantle surface (dependant on the radial position), the pressure forces (p) at the front and rear areas and the gravity force, is the following:

$$-\frac{dp}{dx} + \frac{2}{r}\tau + \rho g = 0 \quad (8)$$

where g is the acceleration of gravity, ρ is the density of the oil and the shear stress (τ) can be defined by the Newton's viscosity law in terms of the velocity of the fluid $u(r)$ and the dynamic viscosity η :

$$\tau(r) = \eta \frac{du(r)}{dr} \quad (9)$$

Establishing the boundary conditions as the following, we can solve the differential equation by separation of variables (see Annex B):

$$p(0) = p_0 + \rho gh \quad p(l) = p_0 \quad u(r_0) = 0 \quad (10)$$

where p_0 is the atmospheric pressure, obtaining:

$$u(r) = \frac{\rho g (l + h)}{4 \eta l} (r_0^2 - r^2) \quad (11)$$

Integrating the velocity for the section of the exit of the syringe (see Annex B), we obtain this result (Hutter and Wang, 2016):

$$Q = \pi \frac{\rho g (l + h)}{8 \eta l} r_0^4 \quad (12)$$

The volumetric flux (Q) can be experimentally calculated by timing the emptying of the syringe, as it is the relation between the volume of the container and that time (t):

$$Q = \frac{V}{t} = \frac{h_e \pi \left(\frac{D}{2}\right)^2}{t} \quad (13)$$

So, rearranging the equation, we can show the dynamic viscosity (η) in terms of the time (t) and a number of parameters that are already known. Therefore, the aim of the experiment is to measure the emptying time of the syringe, to estimate the viscosity:

$$\eta = \pi \frac{\rho g (l + h) t}{8 l (h_e \pi \left(\frac{D}{2}\right)^2)} r_0^4 \quad (14)$$

The classification of the oil is based on the kinematic viscosity, which can be related to the dynamic viscosity on the following way:

$$\nu = \frac{\eta}{\rho} = \pi \frac{g (l + h) t}{8 l (h_e \pi \left(\frac{D}{2}\right)^2)} r_0^4 \quad (15)$$

Results for the high temperature experiment

We have already mentioned that the high temperature experiment is just to make sure that the experiment itself is useful. The viscosity of the oil at $T=25$ °C should be 350 cSt and the experiment will take place at $T=18$ °C. So, the expected value should be slightly above 350 cSt.

The mean value of the times of Table 2 is $\bar{t} = 59.1525$ s and the mean squared error (Márquez and del Río, 2016):

$$\Delta t = \sqrt{\frac{\sum_{n=1}^8 (t_n - \bar{t})^2}{56}} = 0.167404 \text{ s} \quad (16)$$

Table 2: The time needed to empty the syringe from the tenth to the second mark at each of the eight tries of the high temperature experiment. The instrumental error of the timing is 0.01 s.

Experiment n ^o	Time (s)	Experiment n ^o	Time (s)
EXP 1	59.66	EXP 5	59.22
EXP 2	58.40	EXP 6	59.60
EXP 3	59.17	EXP 7	59.10
EXP 4	58.53	EXP 8	59.54

So, the experimental result for the emptying time of the syringe at high temperature is:

$$t = 59.2 \pm 0.2 \text{ s}$$

From this result, we can calculate the viscosity from the equation (15):

$$\nu = 394.091 \text{ cSt} \quad (17)$$

Once we have a result, the propagation of the error of the measurements must be studied:

$$\Delta\nu = \sqrt{\left(\frac{\partial\nu}{\partial h}\right)^2 (\Delta h)^2 + \left(\frac{\partial\nu}{\partial l}\right)^2 (\Delta l)^2 + \left(\frac{\partial\nu}{\partial r_0}\right)^2 (\Delta r_0)^2 + \left(\frac{\partial\nu}{\partial h_e}\right)^2 (\Delta h_e)^2 + \left(\frac{\partial\nu}{\partial D}\right)^2 (\Delta D)^2 + \left(\frac{\partial\nu}{\partial t}\right)^2 (\Delta t)^2} \quad (18)$$

The instrumental error is 0.01 millimeters for all the measurements of the dimensions of the syringe, but, when timing, the references are the ten marks of each milliliter. Therefore, the experimental error of h and h_e will be better estimated by the distance between two marks, instead of by the instrumental error, 0.01 mm. This distance is 7.04 mm, but as the error must only use one meaningful decimal, $\Delta h = 7$ mm. So, the two measurements will be: $h = 70 \pm 7$ mm and $h_e = 52 \pm 7$ mm. The value of acceleration of gravity used will be $g = 9,806.65$ mm/s² (Lascurain et al., 2000) and is taken as a constant, as its error is negligible.

If we develop the expression (18):

$$\Delta\nu = \frac{g}{2} \sqrt{\left(\frac{tr_0^4}{h_e D^2 l}\right)^2 (\Delta h)^2 + \left(-\frac{tr_0^4 h}{h_e D^2 l^2}\right)^2 (\Delta l)^2 + \left(\frac{4(l+h)tr_0^3}{h_e D^2 l}\right)^2 (\Delta r_0)^2 + \left(-\frac{(l+h)tr_0^4}{l D^2 h_e^2}\right)^2 (\Delta h_e)^2 + \left(-\frac{2(l+h)tr_0^4}{lh_e D^3}\right)^2 (\Delta D)^2 + \left(\frac{(l+h)r_0^4}{h_e D^2 l}\right)^2 (\Delta t)^2} \quad (19)$$

It gives the following result:

$$\Delta\nu = 64.7043 \text{ cSt} \quad (20)$$

So, the experimental result for the kinematic viscosity of the oil at high temperature is:

$$\nu = 390 \pm 60 \text{ cSt}$$

As we expected, we get a high error. Anyways, the value of the viscosity is around what we expected. The theoretical value at $T=25$ °C is 350 cSt, so the value being slightly

higher at $T=18$ °C is inside what it was expected. This results encourage us to trust the experiment for the low temperature case.

Results for the low temperature experiment

Once we have concluded that the experiment can be used to correctly estimate the viscosity of the fluid, we are going to repeat the experiment at low temperature. As the temperature of the cold laboratory can oscillate in a margin of several grades, the temperature will be measured alongside with the time for each try of the experiment.

The mean value of the times of Table 3 is $\bar{t} = 82.0973$ s and the mean squared error is:

$$\Delta t = \sqrt{\frac{\sum_{n=1}^{15} (t_n - \bar{t})^2}{210}} = 0.318279 \text{ s} \quad (21)$$

Table 3: The time needed to empty the syringe from the tenth to the fifth mark and the temperature at each of the fifteen tries of the low temperature experiment. The instrumental error of the timing is 0.01 s and the error of the temperature is 0.1 °C.

Experiment n ^o	Time (s)	Temperature (°C)	Experiment n ^o	Time (s)	Temperature (°C)
EXP 1	79.73	-19.4	EXP 9	80.78	-22.5
EXP 2	81.54	-22.3	EXP 10	83.96	-22.8
EXP 3	82.36	-23.0	EXP 11	81.46	-21.4
EXP 4	82.21	-21.5	EXP 12	83.78	-22.5
EXP 5	82.23	-21.4	EXP 13	82.32	-21.5
EXP 6	82.95	-21.9	EXP 14	82.67	- 22.4
EXP 7	81.60	-23.2	EXP 15	83.58	-23.2
EXP 8	80.29	-21.0			

So, the experimental result for the emptying time of the syringe at high temperature is:

$$t = 82.1 \pm 0.3 \text{ s}$$

From this result, we can calculate the viscosity from the equation (15):

$$\nu = 888.120 \text{ cSt} \quad (22)$$

Once we have a result, the propagation of the error of the initial measurements must be calculated with the equations (18) and (19). Which give the following result:

$$\Delta\nu = 211.457 \text{ cSt} \quad (23)$$

So, the experimental result for the kinematic viscosity of the oil at low temperature is:

$$\nu = 900 \pm 200 \text{ cSt}$$

Although the error is huge, the result is close to what we were expecting. So, we can conclude that the dimethicone 350 cSt was a good choice which will lead to a proper viscosity for immersion microscopy.

Both the refraction index and viscosity have been foreseen *grosso modo*, because the main ambition of this work is not a precise quantification of the properties of the dimethicone oil at low temperature, but to evaluate if it approaches the characteristics of the Leica oil. Once this has been fulfilled, looking for a further precision in those measurements is left as an option to a future development of this work.

Once those challenges have been evaluated a number of foreseen advantages and disadvantages can be enumerated related to different aspects of the immersion microscopy on ice:

- One of the main motivations for using the immersion microscopy was that a higher resolution is expected. As the numerical aperture is directly related to the refraction index and a high NA leads to a high resolution, the resolution given by the dimethicone at low temperature ($n_{350(cold)}=1.4246$) will be lower than that given by the Leica Type N immersion oil at $T=23\text{ }^\circ\text{C}$ ($n_N=1.5180$). But, as it may still be much higher than the resolution of an air objective, it will be useful to evaluate the improvement of the resolution.
- Due to a much smaller working distance⁴ for the oil objectives (HC PL FLUOTAR 63x/1,30 OIL WD=0.16 mm) than for the air objectives (HC PL FLUOTAR L 50x/0.55 WD=8 mm and HC PL FLUOTAR L 100x/0,75 WD=4.7 mm), it is not possible to observe the bottom surface of the ice sample with immersion microscopy. When the ice structure 1.1.1 was explained, it was mentioned that the grain boundaries are only observable at the surfaces, so if the bottom is no longer available with this technique, we can only study the grain structure at the top surface.
- The refraction index of hexagonal ice at $T=-22.5\text{ }^\circ\text{C}$ is $n=1.3113$ for light with a 546.1 nm wavelength (Onaka and Kawamura, 1983). This makes the refractive index of ice and dimethicone very close to each other, so the refraction of their common surface will be very low. This leads to a lower background distortion when studying inner structures but, at the same time, makes it very difficult to observe the surface itself.
- Immersion microscopy is said to reduce reflections of incident light coming from spurious sources. So, if we are having trouble with reflections in our lab, it might turn out to be an easy solution.
- Finally, once they have been observed, in order to preserve them at the exact point where were observed, the samples are stored protected by an oil layer. If, in any case, those stored samples have to be reanalyzed, using the oil immersion microscopy with this existing oil seems quite a straightforward procedure.

⁴**Working distance:** maximum distance between the lower bottom of the objective and the surface of study when this is on focus

2.2 Methodology to study ice structure by immersion microscopy

The aim of this project is to develop an immersion microscopy technique on ice, which implies, not only evaluating its viability and results, but also describing the procedure in detail, so that it can be replicated or used by other scientists on their own studies. Indeed, many fronts of this work may offer an option for further study so this section may help whoever is looking for further improvements.

Before even starting to work with the ice, some safety warnings must be given. The working environment is kept below $-20\text{ }^{\circ}\text{C}$ and a relative humidity around 40%. As the work in the cold laboratory may be quite static, you need to wrap up yourself warm and get out of the cold room frequently. Another problem is the humidity that every person perspires, as at such conditions, it tends to immediately condensate and crystallize on any surface, including clothing around the mouth and nose, the scientific instruments or even the samples. Therefore, we also need to be careful with our own breath. Also it must be taken into account that the oils and scientific instruments need some time for acclimatization as we need them to be in a stable condition and cannot be used immediately after taking them inside the cold room. Finally, the installations of the laboratory include an acclimatization chamber to avoid large temperature and humidity changes when someone gets in or out.

Once the caution warnings have been stated, we are now able to make it into the laboratory and start developing the methodology of the immersion microscopy on ice.

2.2.1 Determining the aim of the study and the cut

The first steps of the procedure will be related to the sample. The ice cores coming from high mountain regions or polar areas are stored at around $-70\text{ }^{\circ}\text{C}$ to avoid any alteration on them. Those cores are characterized by their original location and depth. Once the ice core has been evaluated and we have decided the part that we want to observe at the microscope, including its orientation, size and shape; it is time to cut the sample. A vertical electric band saw (see Figure 7) is often used and therefore the safety protocols need to be respected, which include gloves and protective glasses. Moreover, the saw is provided with an adjustable guide which helps to achieve the size we are looking for, besides offering support that helps to avoid abrupt movements of the sample. Finally, we should avoid directly touching the ice piece that we are cutting; to keep the hands far from the saw to avoid accidents. For this purpose we use a plastic bar to move the sample around the saw.



Figure 7: The vertical electric saw used at the IzotzaLab to cut ice. Approximate dimensions: 50x70x160 cm.

The size of the final sample needs to be smaller than the sample holder. In our case, the rectangular ice sample should not be bigger than 4 centimeters wide and 6 centimeters long. The larger the proportion between the length and the width, the greater the risk of

breaking the sample during the preparation, so, ideally the sample should be close to a square shape. In order to give some indications on the third dimension, when we cut the sample at the saw, it should be slightly thicker than a centimeter.

2.2.2 Preparation of the sample

The ice sample, already cut in a suitable size and shape, needs to be conveniently prepared so it can be studied. This means that the ice piece we have just cut needs to become an observable sample, stored at a sample holder and with a smooth surface.

We are going to start from the surface that will end up being the lower surface at the final disposition of the sample. The short working distance of the immersion objective makes it impossible to study this surface by immersion microscopy, so its preparation can be slightly easier because it needs no fine polishing. The ice section is initially placed on the sample holder with this first surface upwards (that is, the section upside-down). Every time we are manipulating the sample, we have to be very careful to avoid contaminating the ice with our body condensation. To attach the ice to the sample holder, we take advantage of the low temperature of the laboratory, and simply use water drops as if it were a kind of "super glue" (the water drops freeze almost instantly). The water dropped from a pipette at the edge of the ice section crystallizes rapidly, attaching the ice and the sample holder together. We need to put a lot of care in those drops, because we do not want the new artificial ice from the drops to contaminate the surface of the sample. The pipette is brought inside the cold laboratory just before we use it and is kept in the pocket, to avoid water freezing inside the pipette itself.

The original surface, produced by cutting with the vertical saw is still rough with saw marks, so in order to place it properly in the final disposition of the sample, it has first to be smoothed out. For this purpose a microtome is used (see Figure 8). This tool is provided with a surgically sharp blade that allows scraping very thin layers and irregularities from the sample. The sample holder with the ice on it will be attached to the plate of the microtome, once again using water to "glue" the sample holder and the plate. By repeatedly performing the microtoming, we can get rid of the surface irregularities until we get a smooth and regular result.

Despite the precision of the microtome, the blade might still leave tiny microscopic scratches on the ice surface. The most prominent parts of these scratches are more exposed and suffer more sublimation. So, time makes those scratches disappear. In practice, 20 minutes are usually enough for this sublimation smoothing in the conditions of the laboratory.

Once the first surface has been properly treated, we can detach the sample holder from the plate of the microtome and the sample from the sample holder, using an auxiliary saw scalpel. Avoiding to damage the sample, we also have to remove the artificial ice drops that we created to "glue" the different elements. In order to avoid over-sublimation at the first surface, it is covered with a thin layer of silicone oil to stop sublimation. This ice section is thus inverted with the already processed and oiled surface placed facing the sample holder, in its final disposition and once again we use the water pipette to attach the ice and the sample holder in the final disposition shown in the Figure 11a.

This upper surface is the one that will be studied with the microscope. Once again the sample holder is attached to the plate of the microtome and scraped with the microtome until we get a smooth surface. This last microtoming session also allows us to obtain the desired thickness of the ice sample. Normally, a thick ice section should be between 5 and 10 millimeters thick at the final step. Thin ice sections can be less than one millimetre thick. When the second surface suits our expectations of thickness and smoothness, it is time to let it sublime. Unlike with the previous surface, this time the sublimation time will be longer. The aim of this sublimation is not only to eliminate the microscopic scratches of the microtome blade, but also to allow the visualization of grain boundaries and sub-grain boundaries, by allowing the formation of surface grooves around these structures as it was explained at the end of Section 1.1.1. At the IzotzaLab, two hours of sublimation may be enough for this purpose.



Figure 8: The microtome used at the Izotzalab. Approximate dimensions: 50x25x30 cm.

As the sample is currently ready for observation with "dry" objective lenses, we can put the combination of sample and sample holder directly on the microscope even during the sublimation process. In this way, we can observe the evolution of the sublimation. Even if the first observations of this process are usually not very useful for microstructure analysis, they might provide some early clues about the sample.

2.2.3 Selection of a point of interest using traditional objective lenses

Due to the difficulties of the use of the oil objectives, the immersion microscopy on ice was proposed as a complementary resource of the traditional "dry" microscopy. Once the oil has been used the image quality obtained by "dry" objectives will decrease, because we have added a new layer that leads to more refraction. So, ideally, the inspection by air objectives will precede the immersion microscopy. Ice samples are often microscopically mapped first, to keep a general record of its microstructure (see Figure 9). If we are working with that aim, this mapping of the whole sample should be done with a traditional "dry" objective. If we are looking for particular structures a general view of the sample looking for those structures should also be done using the "dry" objectives. In both cases, traditional microscopy will be used to identify and locate structures that are worth studying in detail. For this aim, we will use two different objective lenses, with 50x and 100x magnifications, shown in the figures 10a and 10b.

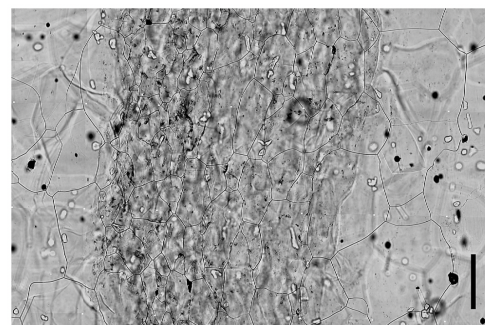


Figure 9: Microstructure-mapping mosaic image the EPICA-DML ice core (depth: 1093 m). Scale bar: 1 mm. (Faria et al., 2010).



Figure 10: Air objective lenses: HC PL FLUOTAR L 50x/0.55 and HC PL FLUOTAR L 100x/0.75 (Leica-Microsystems) and (Leica-Microsystems).

2.2.4 Applying the oil and observation by an immersion objective lens

Once the zones and aims of study for the immersion microscopy have been fixed, we can go on using the oil. The nosepiece of the microscope has several "dry" objectives alongside with the immersion one. For this part of the procedure, we are going to select the oil objective and set it out of focus, just above a point of interest, in order to let space between the sample and the optics. Using a pipette, we are going to put several drops of the oil in the area and submerge the objective into the oil (see a scheme of the set-up in Figure 11a).

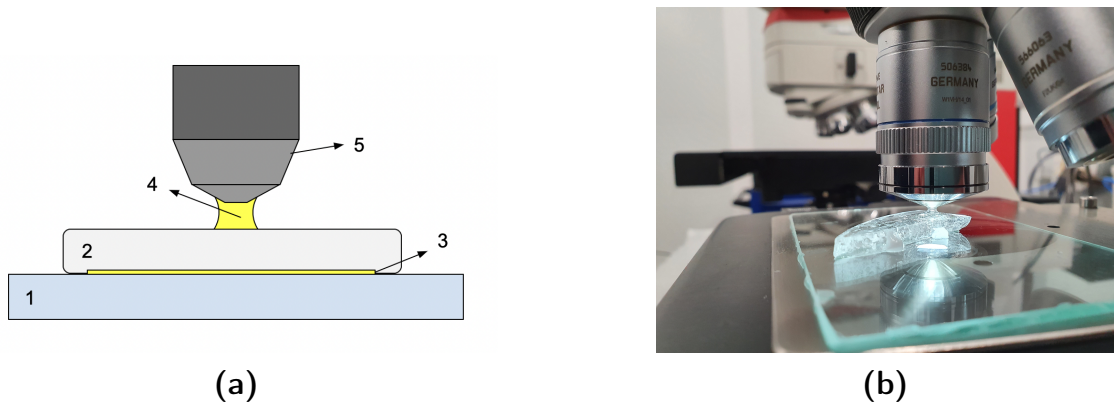


Figure 11: Illustration (a) and image (b) of an ice sample at the microscope and the formation of the meniscus (1-sample holder, 2-ice sheet, 3 and 4-oil, 5-objective).

When we are setting the sample in focus, we need to put caution on the working distance. If we take the sample and the objective far apart the meniscus could break and eventually the objective will get out of the oil. On the other hand, as the working distance of the immersion objective is really small, there is a risk of coming too close and touching the ice. The objective is provided with a coverglass to avoid major damage on the optics, but the sample might also be damaged or contaminated in case of collision.

As the structures that we want to study have already been localized by traditional "dry" microscopy, immersion microscopy does not need much horizontal moving, which will help preserve the meniscus. In case of several points of interest in the same region, a larger amount of oil will be needed; an amount that is enough to keep the objective submerged without allowing the meniscus to break.

2.3 Results of immersion microscopy and comparison with traditional microscopy

Once a procedure has been set to use the oil immersion microscopy in the context of the study of the microstructure of ice below $-20\text{ }^{\circ}\text{C}$, we are aware of the extra difficulties that have appeared with this new method; but time has come to discuss which context or aim of study provides such improved results that justifies to overcome those difficulties. In other words, its time to evaluate the results of the method and its advantages.

This evaluation does not only include a comparison between the traditional ("dry") and immersion objectives, but a number of additional factors that will be analyzed, including the illumination, the use of a polarizing filter and if we are either studying surface or inner structures of the ice. Initially, we also wanted to compare the quality of colour versus black and white photomicrographs, but we rapidly concluded that there was no difference, except for aesthetic purposes (in Section C of the Annexes comparisons of colour and grey-scale photomicrographs are provided as examples).

We have previously mentioned that in the era of digital images, the magnification of the optics is not determinant as it can be complemented with digital zoom. What indeed is important is the resolution (that will limit the digital zoom) and the absolute size of the sample that appears in the photomicrograph. These characteristics remain constant for their corresponding objective lenses, and as the photos are rectangular, they will be expressed as two dimensions:

- HC PL FLUOTAR L 50x/0.55 $\rightarrow 261.8 \pm 0.1\ \mu\text{m} \times 196.3 \pm 0.1\ \mu\text{m}$
- HC PL FLUOTAR 63x/1.30 OIL $\rightarrow 207.8 \pm 0.1\ \mu\text{m} \times 155.8 \pm 0.1\ \mu\text{m}$
- HC PL FLUOTAR L 100x/0.75 $\rightarrow 130.91 \pm 0.01\ \mu\text{m} \times 98.15 \pm 0.01\ \mu\text{m}$

Those are the absolute dimensions of all the photomicrographs unless it is specifically mentioned that the image has been cropped for a particular purpose.

We also have to mention that, for simplicity, we have let the imaging software adjust the exposition automatically, which in certain cases leads to overexposed images that had to be edited before presenting them in these work. In the ambition to undo this excessive brightness, some images ended up having more contrast. So it must be taken into account that this it is not a consequence of the technique, but of the treatment of the images.

2.3.1 Surface structures

When we talk about surface structures, the most notable are grain and subgrain boundaries, followed by dislocation walls. As we have previously mentioned, these structures are present all over the ice, but are only observable at the sample surface. On the following images several triple junctions of grain boundaries are shown. The ice samples of these photos are coming from the Pyrenees mountain region, specifically from the Monte Perdido glacier.

The first comparison aims to determine which type of illumination gives better results when observing the surface, the two candidates being transmitted and incident light.

As we can see in the image pairs 12a / 12b, 13a / 13b and 14a / 14b, when the incident light is used the quality of the image is slightly better. This difference can be specially appreciated at the last pair of images, for the 100x objective. Moreover, when the transmitted light is used, the inner structures that are close to the surface lead to notable shadows. Especially the bubble just above the triple junction, which has a dramatic effect on the three cases. The case of the immersion objective is noteworthy, because we already mentioned that due to the refraction indexes of the ice and the oil being so similar, the irregularities of the surface (e.g. grain-boundary grooves) will be fainter and the inner structures (e.g. bubbles) will be more noticeable.

Even if there are many cases still to analyze, we can already tell that these casuistry does not encourage the use of immersion microscopy.

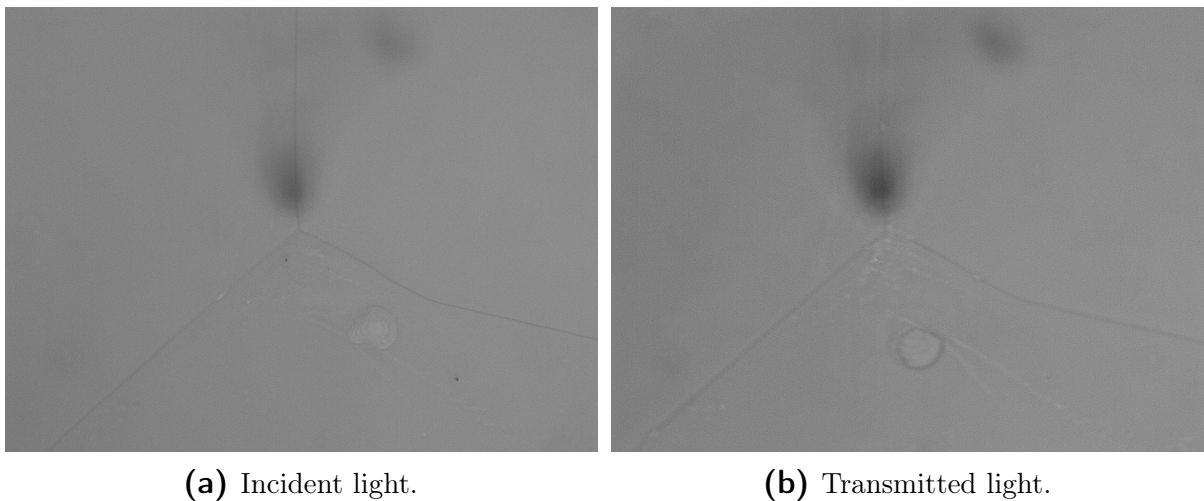


Figure 12: Triple junction observed with the 50x objective lens. Incident and transmitted illumination comparison. It is worth remembering that the width of the area in micrometers is provided in page 25.

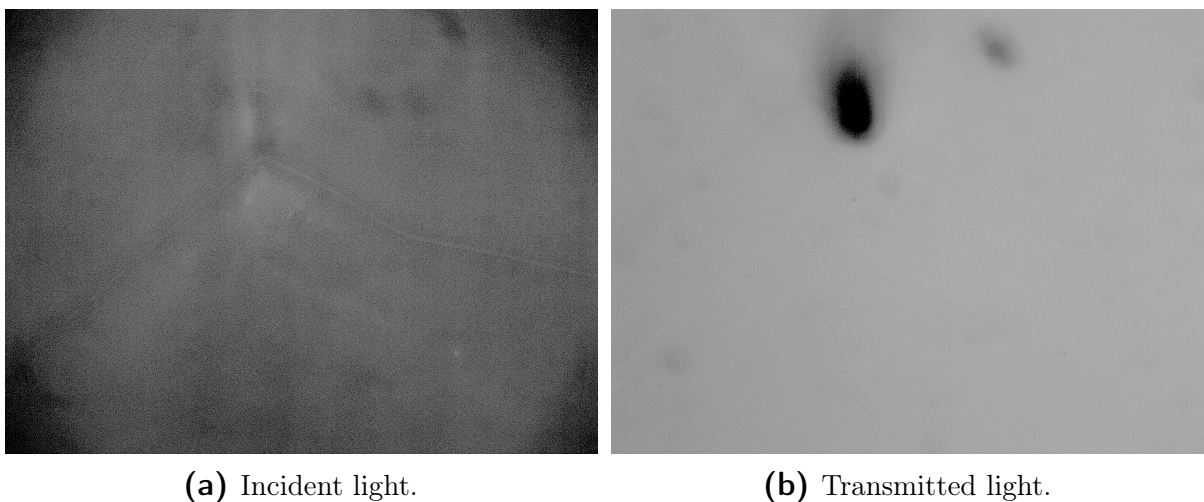


Figure 13: Triple junction observed with the 63x immersion objective lens. Incident and transmitted illumination comparison. It is worth remembering that the width of the area in micrometers is provided in page 25.

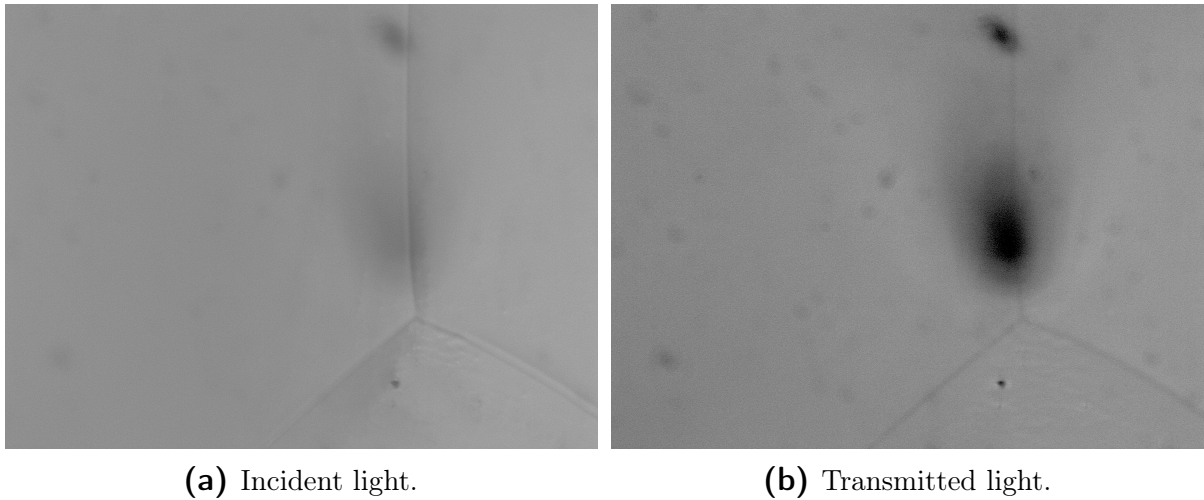


Figure 14: Triple junction observed with the 100x objective lens. Incident and transmitted illumination comparison. It is worth remembering that the width of the area in micrometers is provided in page 25.

Despite the differences, both the transmitted and incident light lead to poor results for all of the objectives. Therefore, we give a try to a combination of both incident and transmitted light. In this case, the transmitted light is set at the minimum and the incident illumination is regulated in order to achieve a correct exposition at the ocular.

If we compare the images 15a, 15b and 16 to those previously analyzed, we can clearly state that the combination of incident and transmitted light gives the best result. In all the cases the background bubble's shadow has been mitigated or even has disappeared for the 50x and 100x objectives. Once again the biggest difference can be appreciated at the 100x objective image, where the details are much sharper at the photo 15b. Once we have agreed that for surface structures the combination of incident and transmitted light is the best option, this will be the standard disposition until the opposite is told.

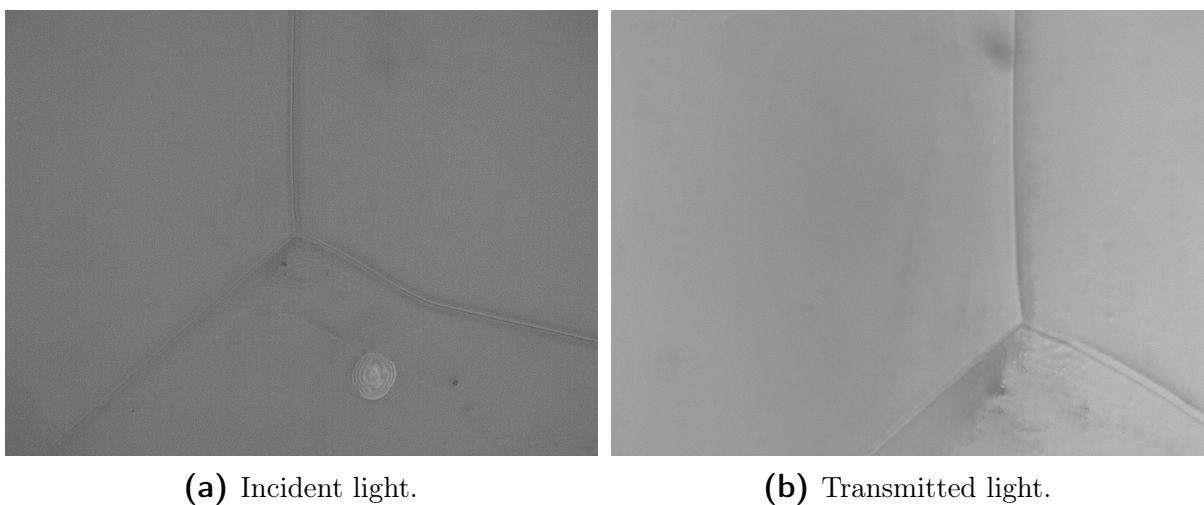


Figure 15: Triple junction observed with the 50x and 100x objective lenses. Both samples are illuminated with both incident and transmitted light. It is worth remembering that the width of the area in micrometers is provided in page 25.

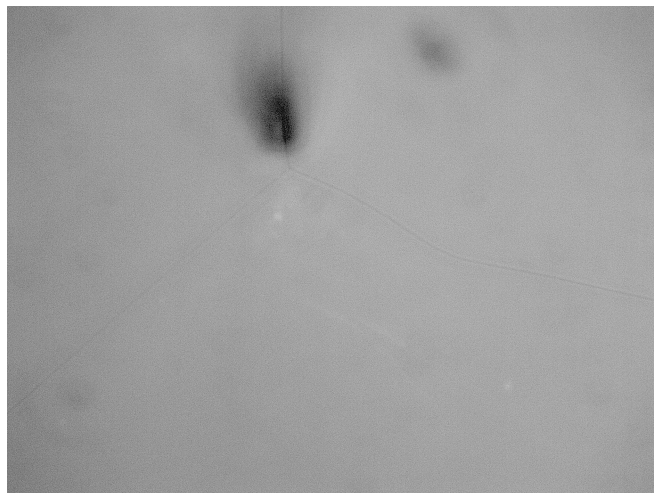
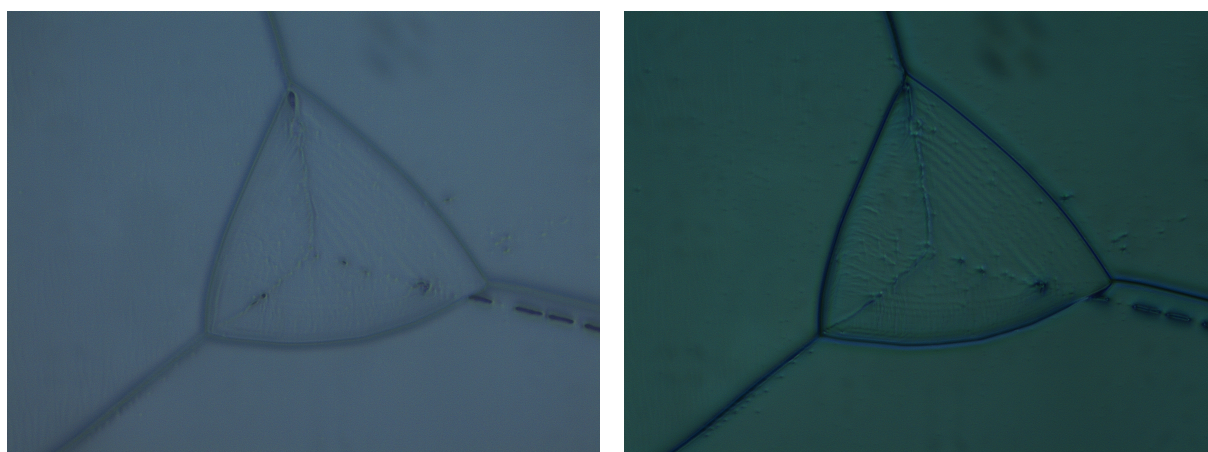


Figure 16: Triple junction observed with the 63x immersion objective lens. The sample is illuminated with both incident and transmitted light. It is worth remembering that the width of the area in micrometers is provided in page 25.

All the images previously studied were taken using a polarizing filter. The next aim of the analysis is to determine if this polarizing filter is conditioning the result. For this purpose we are going to use images from another sample where three triple junctions appear at the same region.

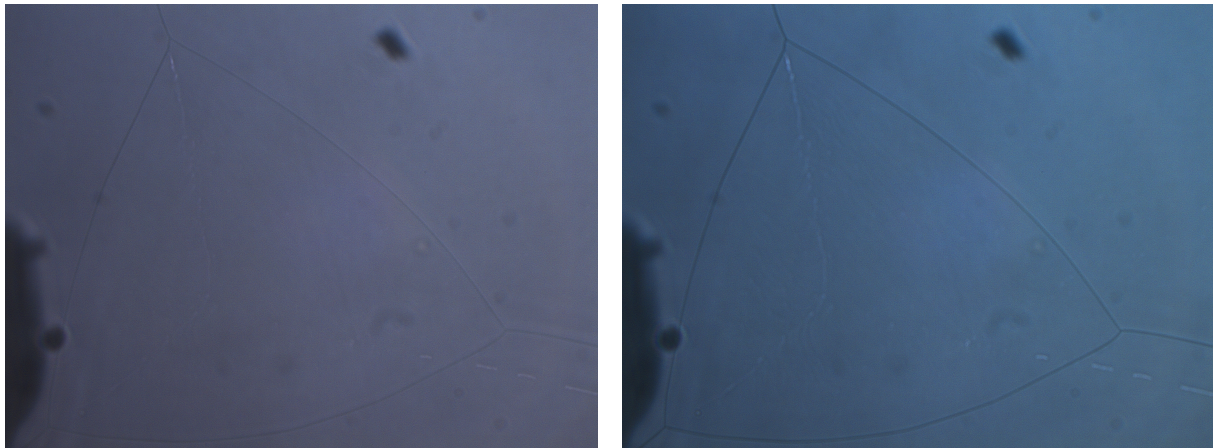
Once again it can be seen in the pairs of images 17a / 17b, 18a / 18b and 19a / 19b that the grain boundaries are much more noticeable when using traditional microscopy than when using immersion techniques. Nevertheless, the point with these photos is to determine how the result can be conditioned by the polarizing filter. Not only with "dry" objectives but also with oil immersion objectives the result is slightly better when the polarizing filter is used. So, since we have arrived to this conclusion, the use of a polarizing filter will be the standard configuration unless the opposite is told.



(a) Without polarizing filter.

(b) With polarizing filter.

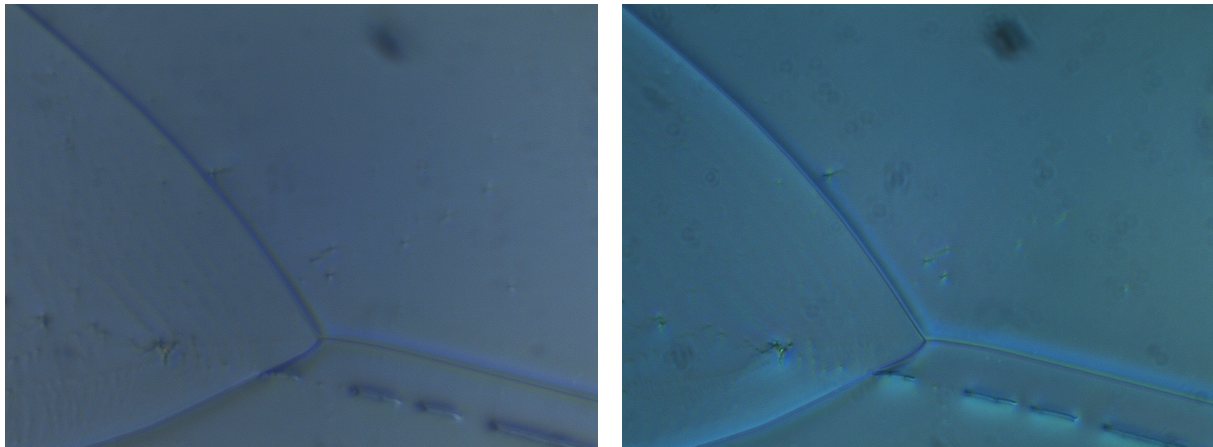
Figure 17: Triple junctions observed with the 50x objective lens. Comparison between using or not using a polarizing filter. It is worth remembering that the width of the area in micrometers is provided in page 25.



(a) Without polarizing filter.

(b) With polarizing filter.

Figure 18: Triple junctions observed with the 63x immersion objective lens. Comparison between using or not using a polarizing filter. It is worth remembering that the width of the area in micrometers is provided in page 25.



(a) Without polarizing filter.

(b) With polarizing filter.

Figure 19: Triple junction observed with the 100x objective lens. Comparison between using or not using a polarizing filter. The width of the area in micrometers is provided in page 25.

2.3.2 Inner structures

Inner structures can include a large variety of inclusions such as bubbles, microparticles, clathrate hydrates or other structures such as slip bands⁵. In the following images we are going to study bubbles, as they are the most common and evident inner structures in our samples.

In a similar way to the previous section, the first aim of these comparisons is to determine which illumination technique leads to a higher image quality. At the same time, we are also going to use the following images to compare the immersion microscopy and traditional microscopy techniques for inner structures. Before going on with this analysis, it is worth remembering that we expected immersion microscopy to show certain

⁵**Slip bands:** A number of parallel layers with high intracrystalline slip activity and many internal defects (mainly dislocations) on the crystal pattern (Faria et al., 2009)

advantages for the observation of inner structures. Indeed we are expecting a higher resolution and less background distortion by the surface structures.

If we study the pairs of images 20a / 20b, 21a / 21b and 22a / 22b, we can clearly see that the transmitted light leads to much better images for any of the three objective lenses. In the case of the "dry" objectives with incident light the bubble can barely be seen and the background distortion of the grain boundaries has a huge impact, as one of the boundary grooves is just above the bubble. For the immersion objective, the image taken with incident light shows the bubble very clearly with a distinctive shape. For surface structures the combination of incident and transmitted light was the best option, so we are giving it a try. The Figure 23 shows the sample when illuminated with both technique and the result is even worse than that of the incident light. Therefore, we can conclude that using only transmitted light is definitely the best option to investigate inner structures.

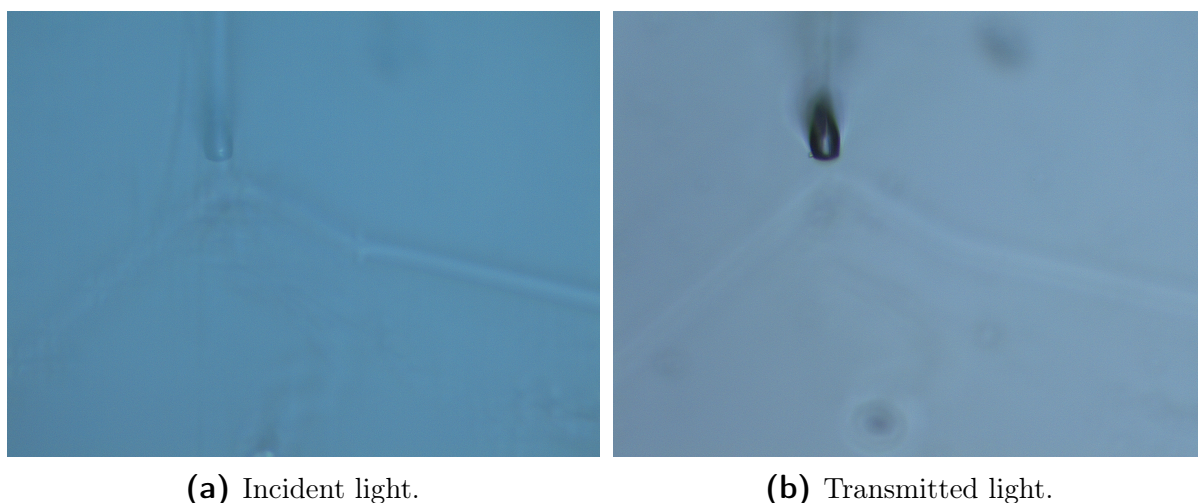


Figure 20: Bubble observed with the 50x objective lens. Incident and transmitted illumination comparison. The width of the area in micrometers is provided in page 25.

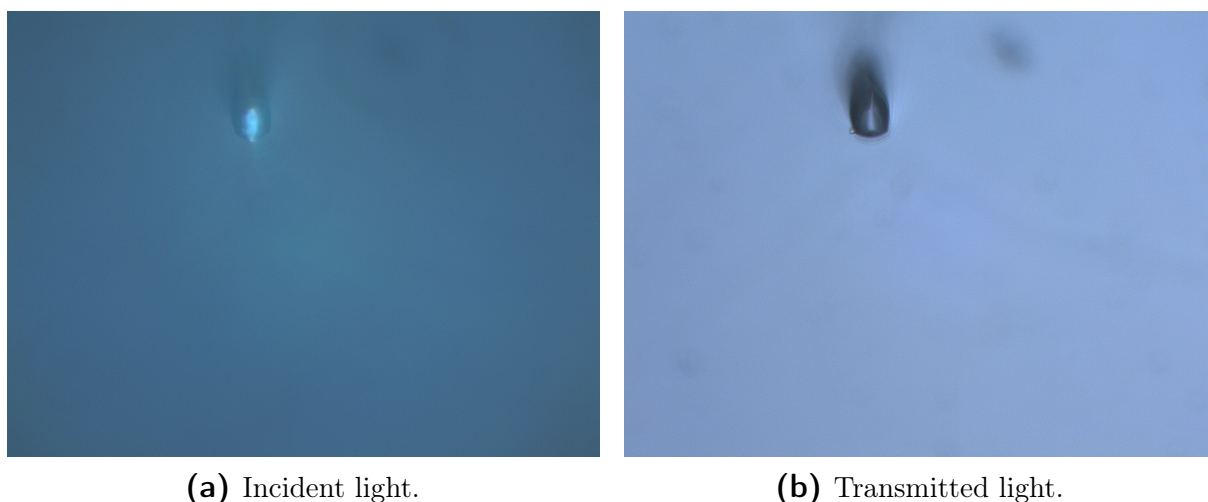


Figure 21: Bubble observed with the 63x immersion objective lens. Incident and transmitted illumination comparison. The width of the area in micrometers is provided in page 25.

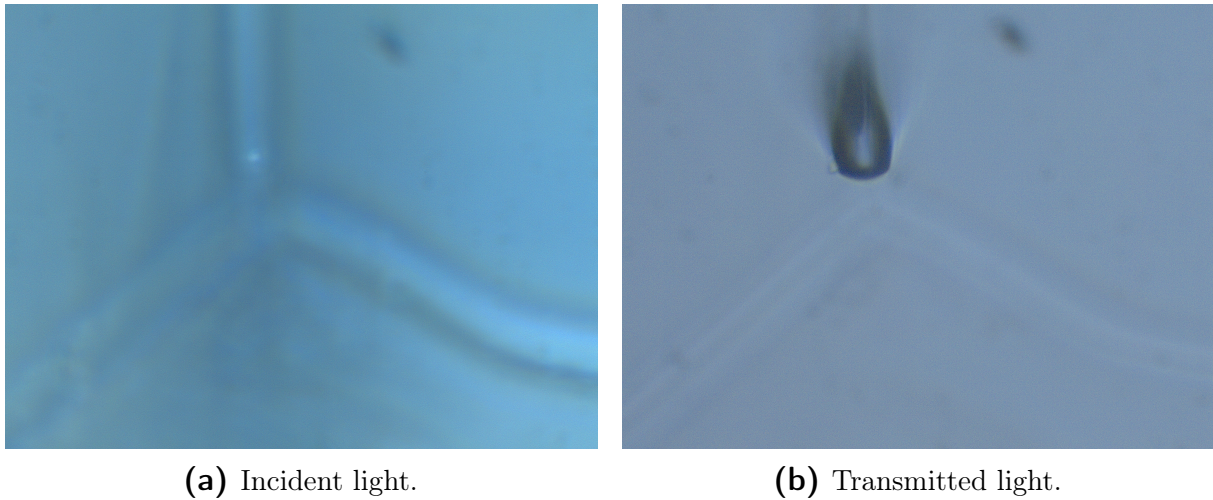


Figure 22: Bubble observed with the 100x objective lens. Incident and transmitted illumination comparison. It is worth remembering that the width of the area in micrometers is provided in page 25.



Figure 23: Bubble observed with the 63x immersion objective lens. The sample is illuminated with both incident and transmitted light. It is worth remembering that the width of the area in micrometers is provided in page 25.

If we compare the best result (transmitted illumination) of the three objective lenses, the most notable difference between the results of traditional and immersion microscopy is how the background distortion originated by the grain boundaries almost disappears for the second one. For the image shown in Figure 21b, the surface structures are almost imperceptible, which is coherent with what we were expecting.

As it happened with the surface structures, all the previous images in Section 2.3.2 were taken using a polarizing filter. In the case of inner structures the use of this filter is not even discussed in this work as it made a little difference in favor of using it, in a similar way to what happened when studying the surface.

In order to reach a conclusion about the resolution of the traditional and immersion microscopy we need to study the images in detail. We have previously stated that the magnification of the optics it is not that important, as in digital image acquisition it can be improved with digital magnification. So, as resolution has nothing to do with magnification, we will compensate the optical magnification with digital zoom on the images shown in Figures 20b, 21b and 22b so the bubble is the same size for the three cases. Also, aiming to make the resolution comparison easier, the images will be cropped, which means that the size of the images in Figure 24 do not coincide with the image sizes defined at the beginning of this chapter.

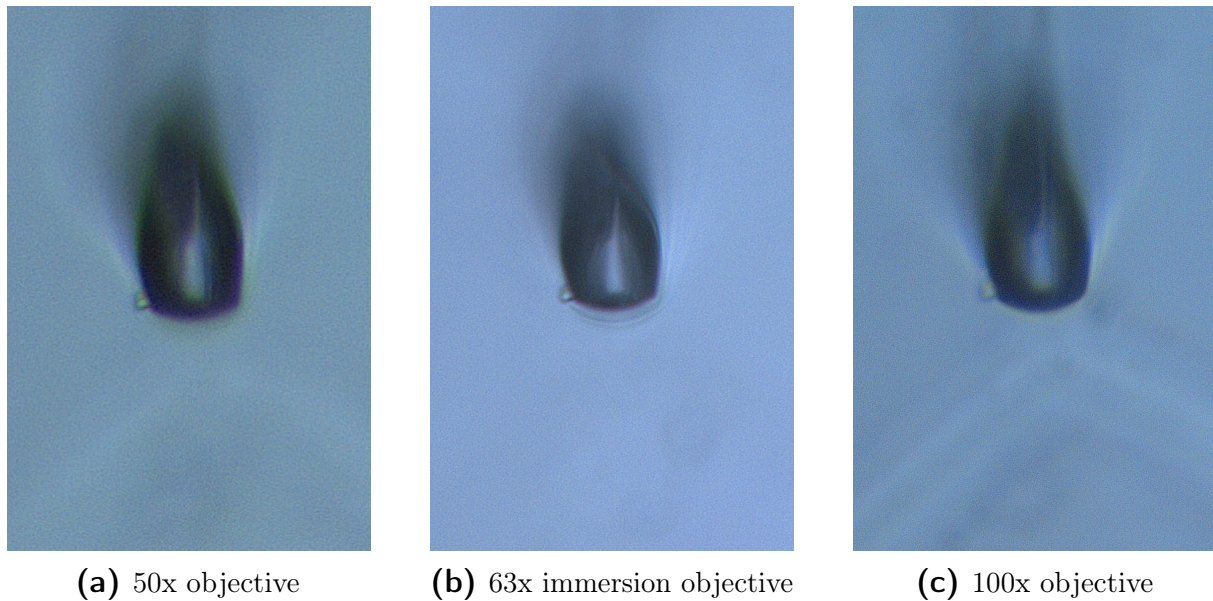


Figure 24: Bubble observed with three different objectives, illuminated with transmitted light. The magnification of the optical devices has been compensated with digital magnification so that the bubble has a similar size for the three images. Therefore, the width of the area is not the one provided in page 25. The dimensions of these photomicrographs are **(a):** $46 \pm 4 \mu\text{m} \times 69 \pm 4 \mu\text{m}$, **(b):** $50 \pm 3 \mu\text{m} \times 75 \pm 3 \mu\text{m}$ and **(c):** $46.2 \pm 0.2 \mu\text{m} \times 69.2 \pm 0.2 \mu\text{m}$

The image shown in Figure 24b, compared to those in Figures 24a and 24c, leaves no doubt about the difference in resolution of the immersion and traditional microscopy. Indeed, on the image obtained with the oil objective all details are much sharper, which proves that we were able to maintain the theoretical advantages on the immersion microscopy for the case of investigating inner structures of the ice, despite the refraction index of the dimethicone 350 cSt at the cold laboratory being notably lower than the index of the Leica Type N immersion liquid at its ideal temperature.

3 | Conclusions

Now that we are facing the end of this work, it is worth the effort of looking back at the proposed objectives in Section 1.3.

First of all, as, to our knowledge, the immersion microscopy technique had never been used to study ice, its viability for ice microstructural studies was the main interest of this work. It can clearly be appreciated at the results that the immersion microscopy has been proven to have certain advantages, specially for the observation of inner structures of ice. A key question is if the use of the oil is worth the complication, but a general answer cannot be given, it would depend on the application. Two main advantages are offered by this technique:

- First, the background distortion derived from surface structures is dramatically minimized when we are observing inner structures. This is due to a lower refraction at the limit between the ice and the outer medium, because the refraction index of the oil is closer to the index of the ice than it is that of the air. This advantage might be specially useful when studying inner interests just under an area with many surface structures.
- Second, the resolution of the images obtained by immersion objectives is notably higher than the resolution of those obtained by air objectives. This was specially observed for inner structures, but should also be a fact for surface images.

Indeed, the study of the ice sample surface by immersion microscopy was highly disappointing, as it offered really poor results. This can be attributed to the fact that the refraction index of the oil ($n=1.4246$) and ice ($n=1.3113$) are too similar at the low temperatures of the cold laboratory. If we had had an oil with an index closer to that of the Leica Type N liquid at $T=25\text{ }^{\circ}\text{C}$ ($n=1.5180$), maybe the study of the surface by immersion microscopy could had given better results.

Nevertheless, the study of inner structures through immersion microscopy gave amazing results. Among the intracrystalline structures that raise interest we can find many types of inclusions, microinclusions and bubbles. The gases at the bubbles and all kind of inclusions such as aerosols, black carbon, ash or pollution particles may give valuable information of the historic composition of the atmosphere, volcanic eruptions or wildfires. In other words, those inclusions are the paleoclimatic record stored in the ice. Moreover, these inclusions are also key factors in order to understand the dynamics of macroscopic ice structures such as glaciers, the poles or the ice sheets of the poles..

In retrospect, these conclusions about the refraction index suggest that a deeper research was worth it in relation to this physical property. This was mainly conditioned by two factors. First, the difficulty to get reliable oils that maintain their properties at low temperatures. Moreover, some of these oils are mainly used in industry and are unlikely to be find at small quantities. Second, we could not find a simple experiment to roughly estimate the refraction index as we did with the viscosity.

On the other hand, the viscosity was deeply studied to clear up the concerns related to it. The viscosity of the dimethicone 350 cSt at the cold laboratory is low enough so

the oil can cover all the sample without making a excessively thick layer and high enough so it does not spread to much, allowing a layer thick enough to immerse the objective and avoiding the oil on the sample to overflow. Additionally, the immersion objective is allowed to move while is immersed. This is a key point of the development of the technique, because it might provide great advantage to observed ice samples that have already been stored. When stored, samples are covered with oil, to avoid over-sublimation, even when immersion oil is not used. But, bringing back those samples to the laboratory and observing the ice section covered with oil through "dry" microscopy gives notably worst results than without the oil. Therefore, immersion microscopy may have a big advantage when it comes to re-observing stored samples.

Even if certain factor affecting the microscopy could not be investigated in depth as desired, this work achieved to analyse a large combination of parameters that affect the observations. The differentiation between black and white and colour images did not awake much interest (see Annex C) and the conclusions about the use of polarizing filters are still preliminary. Nevertheless, the illumination source enriched notably the results of this work. A combination of minimum transmitted light and incident light offered the best results for surface observations while the transmitted light was the best for inner structures. In the last case the illumination was so determinant that any of the observations with transmitted light was much better than the best image among the others, no matter the objective.

In order to come to an end with the evaluation of the technique, the general feeling about it is that it may offer certain advantages, but the extra effort is not worth it for a generalized use. Instead, it has to be understood as a technique complementary to the traditional microscopy. Potentially, one of those particular applications could be the differentiation of slip bands and subgrain boundaries. This could not be tested as we did not have time to scan the samples in search for such structures, but as the technique drastically differentiates surface (subgrain boundary) and inner structures (slip bands), immersion microscopy could be useful to identify such structures and help with what actually is a big challenge when analyzing ice cores by traditional microscopy.

Besides evaluating the usefulness of the technique, this work provides also a detailed description of the methodology, which is not limited to the immersion microscopy on ice, but can be useful for the study of ice by traditional microscopy, as the traditional method is included in this new method (just following all the steps except the last one). Such a detailed methodological description is particularly valuable for future studies, as this work has opened up a number of future lines of research, including a deeper analysis of the effect of the refraction index, the possibilities of polarizing filters or the combination of immersion microscopy with phase-contrast microscopy.

References

- K. Baird, D. Smith, and B. Whitford. Confirmation of the currently accepted value 299,792,458 metres per second for the speed of light. *Optics Communications*, 31(3): 367–368, 1979. 8
- N. B. Barrenetxea and S. H. Faria. Climate change in high-mountain regions: an international perspective and a look at the Pyrenees. *Metode SSJ*, 12:115–121, 2022. 1
- Bayer. *Bayer Silicone Baysilone Öle M.* n.d. (unpublished). 15
- M. P. Bishop, H. Björnsson, W. Haeberli, J. Oerlemans, J. F. Shroder, and M. Tranter. *Encyclopedia of snow, ice and glaciers*. Springer Science & Business Media, 2011. 1, 2
- M. Born and E. Wolf. *Principles of optics: electromagnetic theory of propagation, interference and diffraction of light*. Elsevier, 2013. 9
- DOW. *Technical data sheet: XIAMETER® PMX-200 Silicone Fluid, 50-1,000 CS*. 2017. <https://www.dow.com/documents/en-us/productdatasheet/95/95-5/95-516-xiameter-pmx-200-si-fluid.pdf>. 14, 15
- S. H. Faria. *Crystallization and Recrystallization. Lecture notes*. 2009. (unpublished). 3, 4, 5
- S. H. Faria, S. Kipfstuhl, N. Azuma, J. Freitag, I. Weikusat, M. M. Murshed, and W. F. Kuhs. The multiscale structure of antarctica part i: Inland ice. *Low Temperature Science*, 68(Supplement):39–59, 2009. 29
- S. H. Faria, J. Freitag, and S. Kipfstuhl. Polar ice structure and the integrity of ice-core paleoclimate records. *Quaternary Science Reviews*, 29(1-2):338–351, 2010. 23
- S. H. Faria, I. Weikusat, and N. Azuma. The microstructure of polar ice. part ii: State of the art. *Journal of Structural Geology*, 61:21–49, 2014. 3
- S. H. Faria, S. Kipfstuhl, and A. Lambrecht. *The EPICA-DML deep ice core: a visual record*. Springer, 2017. 2, 4
- F. J. Humphreys and M. Hatherly. *Recrystallization and Related Annealing Phenomena*. Pergamon, Oxford, 2nd edition, 2004. 4, 5
- K. Hutter and Y. Wang. *Fluid and thermodynamics Volume 1: Basic fluid mechanics*, pages 589–592. Springer, 2016. 17
- S. Kipfstuhl, I. Hamann, A. Lambrecht, J. Freitag, S. H. Faria, D. Grigoriev, and N. Azuma. Microstructure mapping: a new method for imaging deformation-induced microstructural features of ice on the grain scale. *Journal of glaciology*, 52(178):398–406, 2006. 5
- J. Lascrain et al. El SI y las leyes sobre pesas y medidas parte I. *Tekhné*, (4):53–61, 2000. 18
- D. Lawlor. *Introduction to light microscopy: tips and tricks for beginners*. Springer, 2019. 10

- Leica-Microsystems. *HC PL FLUOTAR L 100x/0.75*. a. <https://www.leica-microsystems.com/es/productos/objetivos/objectivefinder/objective/566063/>. 24
- Leica-Microsystems. *HC PL FLUOTAR L 50x/0.55*. b. <https://www.leica-microsystems.com/es/productos/objetivos/objectivefinder/detail/objective/566062/>. 24
- Leica-Microsystems. *HC PL FLUOTAR 63x/1.30 OIL*. c. <https://www.leica-microsystems.com/es/productos/objetivos/objectivefinder/objective/506384/>. 11
- Leica-Microsystems. *Technical Information: Type N Immersion liquid*. THORLABS, d. <https://www.thorlabs.com/drawings/946998f39e9eae2-F4D31A31-96F1-08DA-3E58C654332A3B6A/MOIL-20LN-MFGSpec.pdf>. 14, 15
- J. S. Márquez and M. d. P. M. del Río. *Manual práctico para el cálculo de errores en experiencias de laboratorio*. Universidad de Cádiz, 2016. 17
- W. Ockenga. *A Brief Story of Light Microscopy- From the Medieval Reading Stone to Super-Resolution*. 2015. <https://www.leica-microsystems.com/science-lab/a-brief-history-of-light-microscopy-from-the-medieval-reading-stone-to-super-resolution/>. 7
- R. Onaka and T. Kawamura. Refractive indices of hexagonal ice. *Journal of the Physical Society of Japan*, 52(8):2947–2953, 1983. doi: 10.1143/JPSJ.52.2947. <https://doi.org/10.1143/JPSJ.52.2947>. 20
- Químicafácil. *Dimeticona*. 2020. <https://quimicafacil.net/compuesto-de-la-semana/dimeticona/>. 13
- T. G. Rochow and P. A. Tucker. *Introduction to microscopy by means of light, electrons, X rays, or acoustics*. Springer Science & Business Media, 1994. 7, 10, 11
- UNAM. *Determinación del índice de refracción de líquidos*. n.d. <https://www.dow.com/documents/en-us/productdatasheet/95/95-5/95-516-xiameter-pmx-200-si-fluid.pdf>. 14